Pergamon

PII: S0967-0645(96)00058-6

Deep-Sea Research II, Vol. 43, No. 7–8, pp. 1627–1663, 1996
Copyright © 1996 Elsevier Science Ltd
Printed in Great Britain. All rights reserved
0967-0645/96 $15.00 + 0.00

High-resolution observations of plankton spatial distributions correlated with hydrography in the Great South Channel, Georges Bank

SCOTT M. GALLAGER,* CABELL S. DAVIS,* ARI W. EPSTEIN,* ANDY SOLOW* and ROBERT C. BEARDSLEY*

(*Received* 6 *January* 1995; *in revised form* 1 *February* 1996; *accepted* 13 *May* 1996)

Abstract—During a cruise to Georges Bank in May 1992, the Video Plankton Recorder (VPR) was towyoed while non-invasively obtaining images of the plankton and environmental (CTD) data. Data from an 8 h transect across the Great South Channel (GSC) were analyzed on a continuum of spatial scales from coarse-scale (100 km) to micro-scale (mm). Abundance was determined for 12 taxonomic groups including: invertebrate larvae (ophiopluteus larvae, anthozoa larvae: *Cerianthus* sp.), hydroids, copepods (*Calanus* sp., *Pseudocalanus* sp.), pteropods (*Limacina retroversa, Clione* sp.), ctenophores (*Mnemiopsis* sp., *Pleurobrachia* sp.), larvacea (*Oikopleura* sp.), chaetognatha (*Sagitta* sp.), and diatom colonies (*Chaetoceros socialis*).

Species-specific plots of the positions of individual plankton in the water column and plots of the temperature and salinity at which the plankton were observed (temperature–salinity–plankton plots) showed that major taxonomic groups were patchy at coarse scales because of their association with specific water masses of different origin and associated temperature/density discontinuities (pycnocline and fronts). Analysis of the T–S characteristics of water types indicated that diatom colonies and ophiopluteus larvae of echinoderms were transported to GSC in a band of cold water originating on the south flank of Georges Bank. Within this band, diatom colonies formed an intense patch at a front reaching a density of $5\,ml^{-1}$. Within each water mass, fine-scale (10s of meters) plankton patchiness was associated with regions of vertical stability as indicated by the association of plankton with regions of high gradient Richardson number. Aggregation of plankton at the micro-scale (<1 m) occurred significantly only for plankton capable of active swimming, suggesting a dynamic interaction between biological and physical variables at this spatial scale. On occasion, veliger larvae of *Limacina retroversa* were found in spawning patches at concentrations exceeding $600\,ml^{-1}$ within a few centimeters of the air–sea interface. The ability to observe and quantify local concentrations of plankton together with micro-scale physics, but over broad spatial scales, will help provide information on the coupling between spatial scales necessary to understand how individuals interact to form populations and communities in the world oceans. Copyright © 1996 Elsevier Science Ltd

INTRODUCTION

Spatial variability in plankton distributions, and the mechanisms by which it is produced, have been discussed for decades (Bigelow, 1926, 1927; Hardy and Gunther, 1935; Cassie, 1959; McGowan, 1974; Haury *et al.*, 1978). Most studies have been concerned with population abundances at the meso-scale (100–1000 km; Haury, 1976) where spatial integration over large distances by the sampling equipment used was appropriate for the questions being addressed. As advances in sampling technology paralleled an increasing

* Woods Hole Oceanographic Institution, Woods Hole, MA 02543, U.S.A.

interest in variability at smaller spatial scales, new equipment revealed smaller scale plankton distributions to be invariably patchy (Cassie, 1959, 1960; Cushing, 1961; Wiebe, 1970; Owen, 1981). Moreover, patchy distributions of plankton have been found to covary with water column physics within reasonably large (> 100 km) spatial scales (Cassie, 1960; Steele, 1976; Denman and Powell, 1984).

Significant correlations between physical structure and biological structure can arise from both biological and physical sources. Biological sources include behavior in response to the chemical and biological composition of the water column (prey or nutrient localization) or to external environmental forcing (diurnal migration). Physical structuring of the water column can cause redistribution of biology through mixing, or it can isolate biological communities from neighboring water masses. Intrusion of water masses carrying discrete populations has been documented at the meso-scale in a number of studies (e.g. McGowan, 1967; Wiebe *et al.*, 1976). Examples include the distribution and formation of meso-scale eddies, such as Gulf Stream rings in the Northwestern Atlantic, meanders and spin-offs from the loop current in the Gulf of Mexico, broad upwellings and plumes at the shelf break, and the outflow of major river systems. The result of such intrusions can be a significant contrast in biomass and species composition in the plankton over distances of 100s of kilometers. Changes in community composition over smaller scales (coarse-scale: 1–100 km and fine-scale: 1–1000 m) are usually attributed to biological–physical interactions such as accumulation of organisms at fronts and in convective cells due to swimming activity of the plankton (Mackas *et al.*, 1985; Marine Zooplankton Colloquium, 1989). In coastal regions, however, it is often possible to find a number of water types with specific physical properties interacting, mixing and forming a complex three-dimensional mosaic of interleaved water parcels over distances of just a few kilometers. This is particularly true in areas of rapidly changing bathymetry and offshore shoals and banks (e.g. Flagg, 1987).

Given the high degree of variance in plankton biomass often observed at these coarse spatial scales, one can ask how much of the observed biological variance is due to the spatial re-distribution or interaction between specific water parcels within such a mosaic, compared with the variance due to biological factors related to species-specific behavior. To address this question, samples must be taken for physical and biological variables synoptically, and sampling wavelength must be less than one half of the dominant wavelength of the expected changes in water mass and plankton distribution (Denman and Mackas, 1977). Conventional sampling gear precludes such an analysis since nets and pumps tend to integrate sample volumes over greater spatial scales than those necessary to resolve vertical and horizontal boundaries of plankton distributions less than a few 10s of meters. Particle counters, fluorometers, and active acoustic systems allow for rapid data acquisition and processing for particle abundance, size, and chlorophyll levels, but information on the taxonomic composition of the plankton is absent.

With the development of the Video Plankton Recorder (VPR; Davis *et al.*, 1992a), some of these taxon-specific questions as well as questions related to how the distribution of plankton correlates with physical variables on scales from millimeters to 100s of kilometers can be addressed. The VPR is designed to sample non-invasively the micro-distribution and environment of individual plankton over relatively large spatial scales. Fragile forms such as gelatinous zooplankton and colonial phytoplankton are sampled optically in their natural orientation without damage, thus providing information not obtainable by conventional sampling equipment.

The study reported here was part of a pilot cruise in the Global Ocean Ecosystem

Dynamics (GLOBEC) program conducted on Georges Bank in the northwest Atlantic Ocean. The purpose of the GLOBEC Georges Bank program is to understand the mechanisms controlling population size and variability in time and space of key planktonic organisms critical to the fisheries of the region. To this end, the results of a VPR transect made across the Great South Channel (GSC) in May 1992 are reported here. The following questions were addressed.

1. What are the spatial scales for correlation between species-specific distributions of plankton and hydrography?
2. To what extent do water masses provide boundaries to planktonic communities?
3. How important are micro-scale distributions (patchiness) within a given water mass?
4. How does water column stability influence plankton abundance on micro to meso-scales?

METHODS

Physical setting

The Great South Channel (GSC) is a shallow channel (sill depth approximately 70 m) linking the Gulf of Maine to the outer continental shelf and slope of New England (Fig. 1). It is bounded on the east by Georges Bank, and on the west by Nantucket Shoals. Transect VPR 22 was made in the northern GSC, about 50 km north of the channel sill. The transect was conducted on 27–28 May 1992 between 16:20 and 01:30 h local time (EDT) and extended westward 62 km from a starting point at 41°17.3′N, 68°36.80′W. Bottom depth ranged from about 50 m on either side of the channel to > 150 m in the center.

The GSC lies at the intersection of four distinct hydrographic regions: the Gulf of Maine, Georges Bank, Nantucket Shoals, and the outer continental shelf and slope. During late spring, the deep western Gulf of Maine is essentially a three-layer system in which relatively fresh and warm Maine Surface Water overlies the cold Maine Intermediate Water, which in turn overlies the warmer but more saline Maine Bottom Water (Hopkins and Garfield, 1979; Flagg, 1987). In contrast, water over the shallower cap of Georges Bank and over Nantucket Shoals tends to be locally well mixed by strong tidal currents (Hopkins and Garfield, 1981; Limeburner and Beardsley, 1982, 1989). In the late spring, a plume of relatively fresh water, thought to originate in spring runoff from the Penobscot, Kennebec, Androscoggin, and Merrimac Rivers, is found off Cape Cod over the western flank of the northern GSC (Chen *et al.*, 1995a; Limeburner and Beardsley, 1982); the runoff water travels along the western rim of the Gulf of Maine as a buoyant plume, partially mixing with the surrounding water and reaching the northern GSC by mid-May. South of the VPR transect lies a region of relatively well-mixed water covering the sill of the GSC; further south is a stratified region, characteristic of the south flank of Georges Bank, and the Shelf/Slope front. The hydrography of the region as a whole is described by Flagg (1987) and Butman and Beardsley (1987). The northern GSC was studied in some detail during the South Channel Ocean Productivity Experiment (SCOPEX) (Wishner *et al.*, 1988, 1995; Limeburner and Beardsley, 1989; Chen *et al.*, 1995a, 1995b; Durbin *et al.*, 1995a, 1995b; Kann and Wishner, 1995); the transect described here was made in the southernmost region of the SCOPEX study area.

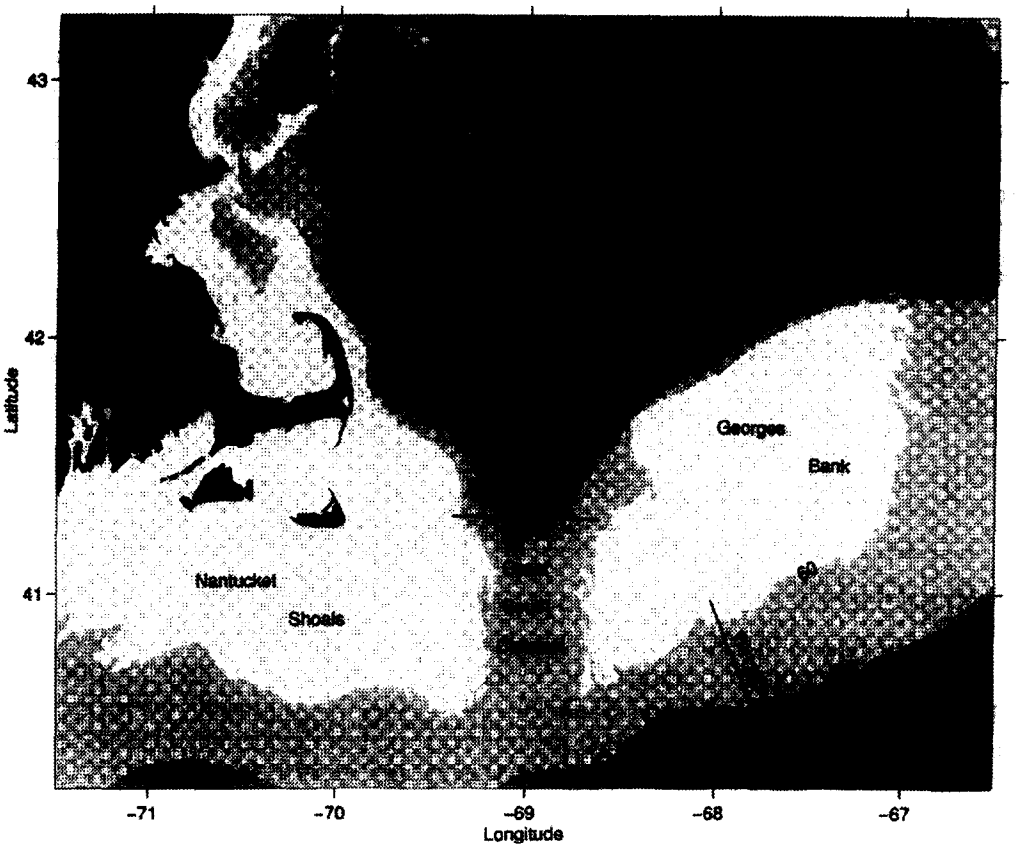

Fig. 1. Overview of the research area with transects VPR 22 and VPR 20 marked.

Sampling techniques

The video plankton recorder (VPR)

The VPR is a towed underwater video microscope with four concentric fields of view (FOV) (a full description of the VPR system is given in Davis *et al.*, 1992a, 1992b). For this cruise, the FOV and imaged volumes (IV) were: Camera 1, $61 \times 40 \times 63$ mm, IV = 154 cm^3; Camera 2, $34 \times 24.5 \times 40$ mm, IV = 33 cm^3; Camera 3, $12 \times 9 \times 20$ mm, IV = 2.0 cm^3; and Camera 4, $6 \times 4.5 \times 23$ mm, IV = 0.62 cm^3. The collimated output from an 80 W xenon red-filtered strobe was synchronized with the video cameras to provide a short (~ 1 μs) light pulse directed at an oblique angle to the cameras. Video data from each camera were transmitted to the surface via fiber-optic cable at 60 Hz and recorded, along with time-code overlay, on high-resolution SONY Betacam SP recorders.

Temperature, salinity, and pressure data were taken by Seabird sensors mounted on the VPR in flow directly behind the imaged volumes. Data were obtained at 10 Hz and averaged over 4 s intervals before being transmitted to the surface. An estimate of the relative uncertainty or noise of the CTD sensors was made following deployment of the VPR at a constant depth (4 m) for 10 min in a well-mixed region of the Bank. The resulting standard deviations are ± 0.046°C for temperature, ± 0.017 psu for salinity, and ± 0.018 for σ_T.

During transect VPR 22, the VPR was towyoed from the air–sea interface to within 10 m of the bottom except in the central portion of the transect, where it was lowered to about 92 m. While the ship steamed in a westward direction at $\approx 2\,m\,s^{-1}$ (4 kts), towyos were produced by winching the cable in and out at a rate of about $0.2\,m\,s^{-1}$. The result was 37 saw-tooth towyo legs or 74 vertical profiles over a horizontal distance of 62 km. At a sampling rate of 60 Hz, the Camera 2 FOV provided nearly contiguous imaged volumes, while the Camera 4 FOV provided non-overlapping imaged volumes at intervals of about 4 cm.

Data processing

Video tapes from cameras 2 and 4 were processed manually field-by-field. The operator scanned slowly (5 fields per second, fps) while looking for in-focus images of plankton. When a target was encountered, the time code and the taxonomic description for the sighting were entered into a data base. In addition, size estimates (length and width) for a few taxonomic groups were recorded from camera 4 images. Each plankton sighting was time-matched with the time in the CTD record and assigned a depth, salinity, and temperature. Accuracy of assigning depth and other variables using this procedure was estimated to be within ± 0.35 m. Sources of error include offset between clocks in the video time code generator and CTD instruments (± 0.25 m) and error due to linear interpolation between CTD data points (± 0.1 m). Sightings of plankton, along with their assigned physical variables, were sorted to the following 12 major taxonomic groups: copepods (*Calanus finmarchicus, Pseudocalanus* sp., other copepods); pteropods (*Limacina retroversa, Clione* sp.); echinoderms (ophiopluteus larvae, metamorphosing juveniles); hydrozoans (*Obelia* sp. and *Clytia* sp.); ctenophores (*Pleurobranchia* sp.); chaetognaths (*Sagitta* sp.); larvaceans (*Oikopleura* sp.); diatoms (*Chaetoceros socialis*).

Coarse-scale (1–10 km) visualization of the biological and physical data on identical spatial scales along the transect required some further processing. Both taxonomic and hydrographic data were interpolated to a regular grid of 300 s × 1 m (~600-m horizontal by 1-m vertical) cells. Plankton abundance was calculated as the number of individuals of a given taxon observed within each 1-m depth bin divided by the total volume sampled in that bin. For example, if 10 copepods were observed in Camera 4 as the VPR traversed a single 1-m depth bin, the abundance of copepods per liter for that bin would be $10/[(0.0006)(60)t]$, where t is the time in seconds between when the VPR entered and exited that particular depth bin. Plots of the gridded cells were completed in Matlab.

To visualize the temperature (T) and salinity (S) in the physical environment of individual plankton within each taxon, and to create what has been called temperature–salinity–plankton (T–S–P) plots (e.g. Michel and Foyo, 1976), T and S values associated with each plankton sighting were binned into cells at intervals of 0.05°C by 0.02 psu, respectively. The normalized plankton abundance was calculated by dividing the sum of the number of plankton of a given taxon in each cell by the total number of individuals of that taxon across the entire transect. To make a T–S–P plot, contour plots of normalized plankton abundance were made directly on a T–S grid. Contours were selected such that they encompassed 95% of the plankton in a given taxon.

To evaluate plankton distributions at the micro-scale (< 1 m), estimates of plankton patchiness were made independently of total plankton abundance using a point-process technique. A patchiness index was calculated for each grid cell intersected by the VPR. For a

single taxon and a single grid cell, let N be the total number of individuals along the VPR transect and let N_i be the number of other individuals in 1 m of the transect of individual i, ($i = 1,2,..., N$). Under a random distribution of individuals, the expected value of N_i is $2(N-1)/L$, where L is the length of the transect through the grid cell. Note that L must be greater than 2 m, otherwise it is not possible to find N_i. In reality, L was about 10 m in most grid cells. The patchiness index (PI) is defined as:

$$PI = (\Sigma N_i/N)/(2(N-1)/L)$$

where the sum is over the N individuals. For each taxon and each grid cell, the significance of PI was calculated by the following simulation procedure. The value of PI was calculated for each of 100 random distributions of N individuals along a transect of length L. The actual distribution was significantly uniform or significantly aggregated if the observed value of PI was below the lower 0.05-quantile or above the upper 0.05-quantile of the distribution of PI generated in this way, respectively.

To evaluate the relationship between plankton aggregation and physical gradients, percentage of the significantly aggregated organisms was plotted against the vertical gradient over 1-m in temperature, salinity, and σ_t in which they were observed. Although the same approach could be used at smaller spatial scales if a sufficient number of observations were available, we used PI to describe patchiness at the 1-m spatial scale only.

Richardson numbers

A key factor in the formation of plankton patches is hypothesized to be the interaction between plankton swimming abilities and the dispersive forces of physical mixing (e.g. Davis *et al.*, 1991; Gallager *et al.*, 1996). As an index of water column stability, gradient Richardson numbers (Ri) were calculated for each grid cell using data on the potential density gradient and shear magnitude according to the formula: $Ri = -(g/\rho)\,(d\rho/dz)/(du/dz)^2$, where g is the gravitational constant, ρ is water density, u is horizontal velocity, and z is depth. In this formulation the numerator is an index of static density stability and the denominator is proportional to the turbulent kinetic energy from vertical shear. A Richardson number equal to or less than about 0.25 indicates the region is susceptible to vertical mixing due to shear instability. Data from the onboard 150-kHz Acoustic Doppler Current Profiler (ADCP) were averaged over 300-s horizontal intervals and 4-m vertical intervals. Vertical shear (du/dz) was calculated by subtracting the velocity vectors in vertically adjacent bins and dividing by the distance between bin centers. Gradients in density ($d\rho/dz$) were calculated from gridded density data smoothed by an 8 m vertical running average. To enable direct comparison, plots of Ri were generated for the same grid cells as the biological and physical data.

RESULTS

General hydrography

The eastern end of transect VPR 22 was at 70 m depth over the western flank of Georges Bank. Here the water was slightly stratified, primarily in temperature (Fig. 2a–c). Moving westward, a sharp horizontal temperature and density gradient, originating at the bottom, was present at about 15 km along the transect. A surface temperature and density front was

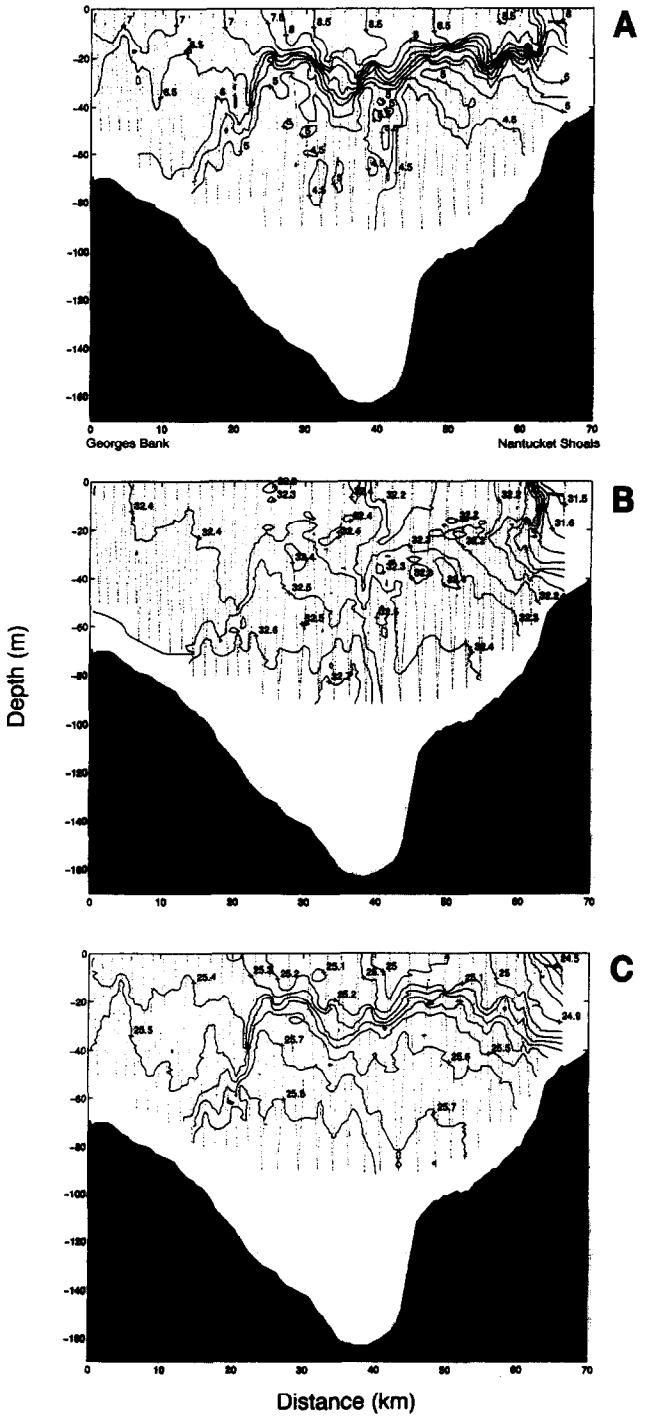

Fig. 2. Temperature (A), salinity (B) and density (C) contours across Great South Channel on 22 May 1992. View is looking south, east-to-west is left-to-right. Each dot along towyo path indicates a CTD data point.

observed at 20 km and joined at 24 km and 20 m depth with the bottom-originating front. This junction formed a pycnocline that continued throughout the rest of the section. The meeting of surface- and bottom-originating isopycnals is a typical signature of a tidal-mixing front (a front formed between a deeper stratified region and a shallower region where tidal currents are sufficiently strong to mix the entire water column). In addition, the appearance of the surface front marked the first location in the transect where σ_t varied vertically by more than 0.5 in the upper 40 m; a $\Delta\sigma_t$ of less than 0.5 in the upper 40 m is the criterion used by Garrett *et al.* (1978) in deciding whether to consider a region tidally well mixed. As we show below, however, a number of distinct water types, having discernible vertical structure, were found in the region to the east of this front; therefore, we do not believe the front was a simple tidal-mixing front.

The bottom of the front coincided with the densest water observed in the transect ($\sigma_T \geq 25.8$). This body of dense water extended westward at least 25 km. (The dense water may have extended farther at depth, but we have information for only the top 92 m, the maximum depth sampled.) At depths above this dense water, but below the pycnocline, the temperature field was not smooth: there occurred a number of intrusions of water that were either cooler ($T \leq 4.5$°C) or warmer ($T \geq 5$°C) than the surrounding water. At the surface, regions of warm ($T \geq 8.5$°C) water alternated with regions of slightly cooler but fresher, and hence less dense, water. This surface pattern extended from the surface temperature front nearly to the western end of the transect.

Between about 38 and 60 km along the transect lay a large body of cold ($T \leq 4.5$°C) water extending from at least 92-m depth to as shallow as about 30 m. This cold water was considerably fresher and less dense than the body of dense water immediately to its east. The body of cold water extended westward about 20 km, until the bottom depth was about 60 m. Above this cold water and below the surface water, the water became fresher toward the west, eventually reaching salinities as low as 31.7 psu. Near the end of the transect, these lower salinities were visible at the surface in a sharp surface salinity front.

T–S *and water-type analysis*

The short horizontal distances between vertical legs permitted an unusually detailed hydrographic analysis of the section. In our initial *T–S* analysis, we treated each of the transect's 74 vertical legs separately. To prevent the analysis from being biased by the varying amounts of time the VPR spent at different depths, the individual temperature and salinity data points for each vertical leg were projected onto regularly-spaced depth intervals (2 m) using a sum of cubic splines calculated to fit the data optimally in a least-squares sense. In order to identify water types that were common to many legs, *T–S* diagrams were plotted for each leg and compared (Fig. 3). Using a composite *T–S* diagram, along with the *T* and *S* data for each vertical leg, a complete picture of the various water masses encountered along the transect was developed (Fig. 4). Although some of the identified water types correspond to water masses expected in this region during spring and summer, others are transient and probably existed in the GSC for only a relatively short time. Moreover, because the transect required a major fraction of a tidal cycle to complete, Fig. 4 does not represent a "snapshot" in time of water mass distribution. Nevertheless, since this figure displays the water types present when the VPR completed each part of the transect, the hydrography is directly comparable with the observed biology at the same times and locations.

The densest water in the section was Maine Intermediate Water (MIW) (Figs 3 and 4),

which occurred at depths below about 60 m between 15 and 40 km along the transect. Having a σ_t generally above 25.8, the MIW shown here had salinities between about 32.5 and 32.75 psu and temperatures between about 4.5 and 4.8°C. Above the MIW was a triangularly-shaped water mass whose T–S properties suggest that it was formed by mixing between MIW and the overlying water.

The coldest water in the section ($T \leq 4.5$°C, S between about 32.3 and 32.6 psu), found over the western flank of the Great South Channel between 38 and 60 km along the transect (see Fig. 2a), was similar in both position and T–S properties to cold subsurface tongues identified in May 1976 and May 1979 sections by Limeburner and Beardsley (1982). Chen *et al.* (1995a) suggested that this cold tongue consists of water (perhaps originating as MIW) that has been freshened and cooled during winter along the shallow edge of the western Gulf of Maine, and which has then flowed southward under the developing seasonal thermocline along the coast into the northern GSC. We shall refer to this water type as Cold Coastal Water (CCW). A few intrusions of CCW were found in the central part of the section at depths of about 65 m, just above the core of MIW.

At the far eastern end of the section (near the western edge of Georges Bank) four distinct water types were identified. We shall refer to them as: Western Bank Water 1, Western Bank Surface Water 1, Western Bank Water 2 and Western Bank Surface Water 2 (WBW1, WBSW1, WBW2, WBSW2). Although WBW1 and WBW2 were similar to each other, as were WBSW1 and WBSW2, they were identified as separate water types because data points for the relevant vertical legs clustered in distinct groups on T–S diagrams (Figs 3 and 4), and because the horizontal transition between these water types was very rapid (it occurred within 2 km). In both the surface water and the intermediate-depth water, the water to the east (WBW1 and WBSW1) was saltier and slightly warmer than the water to the west (WBW2 and WBSW2). The T–S properties of all of these water types could be produced by mixing between MIW and the surface waters found in central and western portions of this section (discussed below). This result is expected since water over the western section of Georges Bank is thought to be formed by tidal mixing between MIW and surface water in the Gulf of Maine (Hopkins and Garfield, 1981; Flagg, 1987).

Surface water in the central and western portions of the section was warmer and fresher than the surface water to the east. It consisted of two parcels of warm water ($T > 8.5$°C) interspersed among two parcels of slightly colder, fresher water. The eastern-most parcel of warm water, which occurred in the center of the transect, was called Channel Surface Water 1 (CSW1). The other parcel of warm water, located between 50 and 55 km along the transect, was called Channel Surface Water 2 (CSW2). The parcels of colder water, which were essentially identical to each other in their T–S properties, were called Channel Surface Water 3 (CSW3). CSW3 was found between 40 and 50 km and between 55 and 62 km along the transect.

The near-surface water at the far western end of the transect was considerably fresher ($S < 31.6$ psu) than water anywhere else in the transect. The physical location and T–S properties of this fresh water led us to believe that it marked the southern extreme of the surface fresh-water plume that forms off of Cape Cod each spring because of runoff into the western Gulf of Maine (e.g. Limeburner and Beardsley, 1982; Chen *et al.*, 1995a). We designated this fresh water Plume Surface Water (PSW).

The fresh surface plume's influence was seen at intermediate depths as well. Beginning at about 48 km along the transect, water at depths between about 15 and 50 m became markedly fresher than the water above or below it, growing increasingly fresh toward the

west. *T–S* plots of the relevant vertical legs (Fig. 3) showed clear evidence of mixing, with some intermediate-depth water having salinity between about 31.55 and 31.75 psu and temperature between about 5.25 and 6°C. This water was designated Plume Intermediate Water (PIW); it was not directly sampled by the VPR. The region where water properties were influenced by mixing with PIW is indicated in Fig. 4.

Analysis of the remaining portions of the section (the two areas labeled "SW/CBW" and the area labeled "Interleaved SW/CBW and SW/MIW") was somewhat more complicated, and relied, in part, on biological information provided by the VPR. The areas labeled "SW/CBW" contained water that seemed to be the product of mixing between the overlying surface water and some cold ($T < 5$°C) water having salinity between 32.3 and 32.5 psu (Fig. 4). The area labeled "Interleaved SW/MIW and SW/CBW" seemed to consist of layers of surface water mixed with that same cold water, interleaved with layers of surface water mixed with MIW (Fig. 4). The Cold Band Water (CBW) was believed to originate in the Cold Band that flowes southwestward along the south flank of Georges Bank. Further interpretation of these results will be discussed after describing the biological results.

Water column stability

Gradient Richardson number (*Ri*) plotted as a function of depth and distance across the transect spanned more than two orders of magnitude (Fig. 5). In general, regions of high *Ri* (high static stability) tended to occur in areas of strong stratification, as would be expected. *Ri* exhibited high spatial variability mainly due to variations in the measured values of shear. On the whole, water masses exhibited smaller *Ri* (i.e. reduced stability) within the body of each water mass and away from interfaces with other water masses. Closer to the boundaries between water masses, *Ri* tended to increase rapidly, suggesting greater vertical stability. This was true for both vertical and horizontal boundaries. (Note relatively high *Ri* values between MIW and CCW at about 40 m along the transect.)

Distribution and abundance of plankton

Identification of plankton to major taxonomic group, and to genus in many cases, was possible from the video images recorded from Camera 4 (FOV = 6 × 4.5 mm). Features such as the number and shape of the seta on the antenna of *Calanus finmarchicus*, the number of whorls in the shells of *Limacina retroversa*, and the number and length of arms of echinoid ophiopluteus larvae were used to characterize individuals from the images. After some experience was gained in making plankton identifications from Camera 4, the larger FOV of Camera 2 (34 × 24.5 mm) was used to identify plankton for estimates of abundance and distribution. Two exceptions to this were for the diatom colonies *Chaetoceros socialis* and *Limacina retroversa*, which were too numerous to count at certain times from Camera 2. Distributions and abundances for each of the taxa will be discussed separately in order of region of occurrence and abundance.

Hydrozoa (Fig. 6A)

Hydroid polyps and free-swimming medusa were strikingly confined to the well-mixed region of the bank. (Although we identified this hydroid as *Obelia* sp. based on the number of tentacles on the medusa [i.e. > 8], the length and diameter of the polyps are similar to those of *Clytia* sp.) The western boundary of the hydroid distribution was distinctly marked

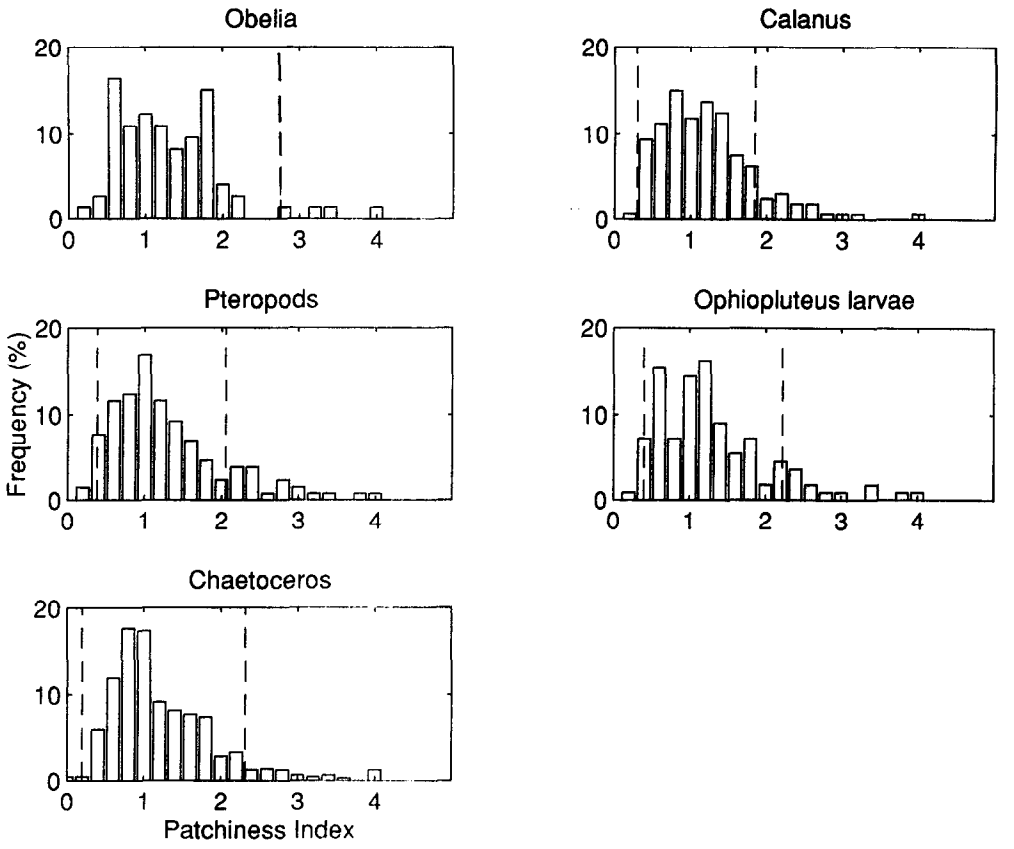

Fig. 7. Frequency histograms for the taxon-specific micro-scale Patchiness Index (*PI*) across VPR 22 generated for each grid cell traversed by the VPR. 95% confidence intervals are shown as vertical dashed lines. Bins above and below the confidence interval show aggregated and uniform distributions, respectively.

by the parabolically-shaped front (separating SW/CBW, SW/MIW, and MIW). On the Bank, few hydroids were found above 10 m where the Western Bank Surface Water masses 1 and 2 (WBSW1 and WBSW2) were identified. Maximum concentration of medusa approached $0.6\,l^{-1}$ in the region of WBW1 water.

The micro-scale patchiness index (*PI*) showed that 94.5% of the medusae and polyps were randomly distributed across the entire transect (Fig. 7). Only 5.5% were aggregated and none were uniformly distributed. Of those hydroids that were aggregated, the tendency was for aggregation within weak temperature gradients (Fig. 8). Data for the other physical gradients showed similar results, so only those for temperature are presented here.

Orientation of individual medusa appeared random with roughly equal possibilities of finding animals in a mouth-up or mouth-down position. Medusae varied in diameter from 1

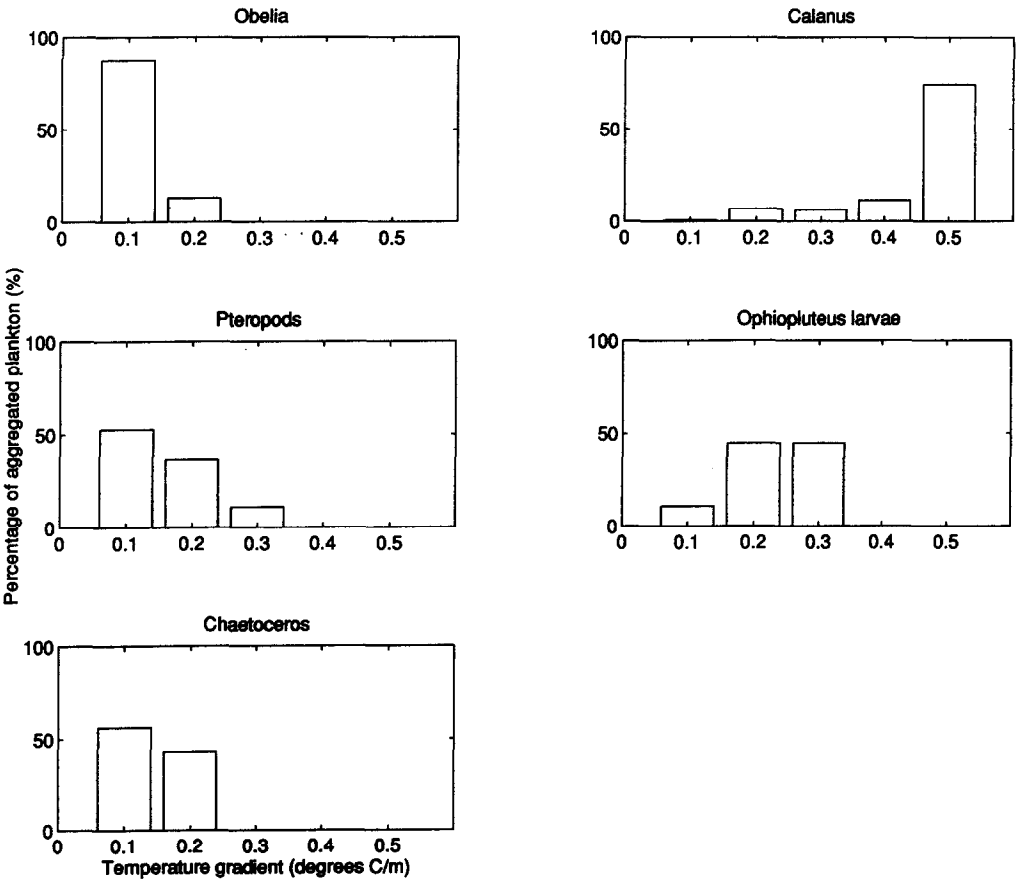

Fig. 8. Percentage of the aggregated organisms in a given population in relation to the vertical gradient in temperature calculated at 1 m intervals. Data are binned at intervals of $0.1°C\,m^{-1}$.

to 2.5 mm. Polyps were found in all orientations with tentacles extended and relaxed in most images.

Calanus (Fig. 6B)

Life stages CV and adult *Calanus finmarchicus* were positively identified from the video images by virtue of their bifurcated antenna (length: 1.2–2 mm). Younger stages (CI–CIV) were identified as *Calanus* only. It is well known from net hauls that nearly all *Calanus* in this region at this time of year are *C. finmarchicus* copepodid stages CIV–CVI (Davis, 1987). For the purpose of obtaining the distributional pattern and average concentration for this genus, all life stages were pooled.

In general, *Calanus* was observed both within and above the thermocline to the west of the front in the CSW 1, 2, and 3. A sharp boundary between CSW3, Plume Surface Water (PSW), and PIW-influenced water indicated that few *Calanus* were in the relatively warm and fresh water influenced by river runoff. A clearly defined patch of *Calanus* was observed

within the thermocline about 45 km from the beginning of the transect. Concentrations exceeding $2.5\,l^{-1}$ on average were found between 15 and 20 m in depth for a distance of about 2 km. In the region of this patch, maximum number of *Calanus* observed in a single field from Camera 2 was 8, indicating a local concentration of about $285\,l^{-1}$.

The micro-scale patchiness index showed that 76.9% of the *Calanus* were randomly distributed, 15.6% were aggregated, and 7.5% were uniformly distributed (Fig. 7). Those that were aggregated tended to aggregate in the strongest temperature gradients (Fig. 8) that corresponded to the thermocline at about 30 km into the transect.

Body orientation of individual *Calanus* was, for the most part, either in the head-up or head-down position. Observations of individuals in a horizontal position with their body axis either orthogonal or parallel to the camera's view were rare.

Limacina retroversa (Fig. 6C,D)

The highly refractive shells of the pteropod *Limacina retroversa* allowed for rapid identification of this spheroid-like organism. The number of shell whorls ranged between two and six as body size increased from 0.5 to 2 mm. *L. retroversa* were found primarily above the thermocline in dense aggregations bounded by the 8.5°C temperature contour to the west of the surface density front, corresponding to water types CSW1 and CSW2, but not CSW3. The concentration at the centroids of these aggregations exceeded $7\,l^{-1}$ and were located well within these water masses rather than near the boundaries. Similar high densities were recorded just below the air–water interface to a depth of 0.5 m. Close to the surface, adult *L. retroversa* were observed releasing embryo ribbons in streamers around themselves. Over 370 embryos (*ca* 200 μm in length) were counted in a single video field of Camera 4, thus yielding a local concentration in excess of $600\,ml^{-1}$.

Micro-scale distributions of adult *Limacina retroversa* were 75.4% random, 15.3% aggregated, and 9.3% uniform (Fig. 7). The predominant number of aggregated *L. retroversa* were found in the weakest temperature gradients (Fig. 8) corresponding to the centers of water masses CSW1 and CSW2.

Body orientation was observed always with the shell below the parapodia relative to the gravity vector. The parapodia, however, were found in varying positions throughout the effective and return strokes of the swimming cycle. No evidence of a feeding mucous web was observed in any of the >9000 images containing *L. retroversa.*

Ophiopluteus larvae (Fig. 6E)

Ophiopluteus larvae were identified by their unequal arm length compared with equal arm lengths found in echinopluteus larvae. The species is unknown, but a number of brittle stars (e.g. *Ophiura sarsi*) and basket stars are present in the Gulf of Maine and Georges Bank region (see Theroux and Grosslein, 1987). Individuals undergoing metamorphosis (shortening of arms toward the main body), were placed in a separate juvenile category.

In contrast to the hydrozoans, which occurred in the tidally mixed area of Georges Bank, ophiopluteus larvae were restricted to the deeper, cooler waters of the Gulf of Maine, and their distributions followed the base of the thermocline. More specifically, they were distributed to the west of the front and below the thermocline in the SW/CBW, SW/MIW, and interleaved SW/CBW and SW/MIW. The western boundary of the larval population was between the MIW and CCW. Although few larvae were observed in the CCW, relatively high numbers ($0.9\,l^{-1}$) were found between CCW and PIW-influenced water on the west side of the channel.

Micro-scale distributions of ophiopluteus larvae were 82.9% random, 13.5% aggregated, and 3.6% uniform (Fig. 7). When aggregated, larvae tended to be found in relatively strong temperature gradients (Fig. 8) at interfaces between water masses.

Larval orientation was consistently in the arms-up position. Very little deviation from this orientation was observed regardless of the hydrographic conditions or mixing intensity.

Juvenile ophiuroids (Fig. 6F)

Metamorphosing juvenile ophiuroids were found well up into the water column, but in general, were distributed at a greater depth than their larval counterparts. Interestingly, low numbers ($0.01\,l^{-1}$) were found in regions where larvae were virtually absent such as the MIW, CCW, WBW1 and WBW2 on the eastern side of the channel.

Diatom colonies (Fig. 6G)

Colonies of the centric diatom *Chaetoceros socialis* were observed in great abundance in specific regions of the channel. The VPR images of the colonies showed globular forms ranging in diameter from 0.5 to 2 mm. Groups of colonies exceeded 5 cm in maximum dimension. Fine structure within the colonies was difficult to see without further image processing. Application of an edge enhancement filter (Sobel; 3×3 kernal) revealed detailed structure consisting of diatom chains formed into "S" patterns throughout an amorphous gelatinous matrix.

Although no water samples were taken on cruise EN237 to verify the identification of this diatom, subsequent cruises to Georges Bank with the VPR have revealed similar forms in abundance. Microscopic examination of Niskin bottle samples taken during those cruises confirmed they were colonies of *Chaetoceros socialis*.

Colonies were abundant ($200–300\,l^{-1}$) on the eastern side of the channel extending from the surface to the bottom (WBSW1, 2 and WBW1 and 2). Within the front, and particularly at a nearby region where isotherms sloped sharply (depth = 55 m, distance = 20 km), the concentration of colonies, averaged over 1 m (depth) by 600 m (distance) bins, exceeded $600\,l^{-1}$. *Ri* in this region tended to be high, suggesting great vertical stability. The VPR video screen displaying images in real-time for Camera 4 literally turned white for a few seconds as the VPR traversed this patch. While in the patch, the maximum number of colonies observed in the Camera 4 FOV was three, giving a local concentration of $5\,ml^{-1}$. The boundaries of the patch were very sharp as the concentration fell by a factor of 100 within 0.5 m above and 5 m below the patch. The diatom patch was encompassed within the water mass identified as SW/CBW. Colonies also were observed at the boundaries between SW/CBW and SW/MIW, and in the region of interleaving between SW/CBW and SW/MIW, but not in the MIW itself. Few colonies were found in the CCW mass to the west (although scattered observations showed low numbers in the region between the CCW and PIW).

The micro-scale patchiness index revealed the majority (92.3%) of diatom colonies to be random in their distributions (Fig. 7). Only 7.2% were aggregated, and 0.5% were uniform. The few that were aggregated were found in the temperature inversion (medium to low temperature gradient; Fig. 8) within the front.

Larvacea (Fig. 6H)

Larvaceans, *Oikopleura* sp., were found encased in a gelatinous house in the majority of

observations. Since positive identification was dependent, in part, on the presence of the house, only those within a house are reported here. Larvaceans were distributed in a pattern similar to that of the ctenophores (Fig. 6N): relatively high concentrations on both the west and east sides of the channel with few in the center. On the east side of the channel, they were found in the WBW1 and 2 regions with a few scattered near the surface in the WBSW1 and 2. On the west side, larvaceans ranged throughout the water column between the PSW at the surface, the PIW-influenced water 20–60 m in depth, and into the CCW below 60 m. No preferred body orientation was observed for *Oikopleura* sp.

Other copepods (Fig. 6I)

This category included the remaining species of copepods along with small and immature stages of *Calanus* and *Pseudocalanus* sp. that, for one or more reasons, were not always identified to genus. Additional copepod species included *Acartia* sp., *Eucalanus* sp., *Metridia* sp., *Neocalanus* sp., *Paracalanus* sp., *Temora* sp., and *Oithona* sp. These groups were most abundant in the well-mixed regions WBS1 and 2, WBW1 and 2, within 20 m of the surface in the CSW1, 2 and 3 water masses, and in the PIW-influenced region between 10 and 30 m depth on the eastern boundary of the channel. As for *Calanus* and *Pseudocalanus* sp., these copepods were also rare in the deep MIW and CCW.

Body orientation in *Oithona* sp. was always in a head-down position. No specific orientations were noted for the other species.

Pseudocalanus sp. (females; Fig. 6J)

Female *Pseudocalanus* sp. (length: 0.9–1.5 mm) were identified by the tight constriction at the urosome and the presence of egg (embryo) sacs attached to the abdomen. The number of embryos in the sac were counted in most images yielding an average of 13 ($n = 108$, SD = 5) per female. Compared with *Calanus*, the abundance of *Pseudocalanus* sp. females was low with only scattered observations throughout WBW, CSW, and CCW. A single dense patch was found near the surface in the well-mixed region in which the local concentration exceeded 3 ml^{-1}.

Body orientation appeared random with no preferential position relative to gravity or the camera axis.

Clione sp. (Fig. 6K)

The large ($\sim$2 cm in length) gymnosome pteropod *Clione* sp. was found in low abundance in the regions of CSW1 and CSW2. Although only scattered observations were made, they were generally found in the same regions as *Limacina retroversa* above the thermocline between 30 and 50 km from the beginning of the transect.

There was no preferred body orientation in the water column.

Chaetognatha (Fig. 6L)

The chaetognath *Sagitta* sp. was rare in most of the channel, with only a few individuals observed during the latter half of the transect. From about 32 km into the transect, *Sagitta* sp. ranged between the surface and 80 m.

Invariably, *Sagitta* sp. was found in a head-down orientation.

Anthozoa (Fig. 6M)

Larvae of the burrowing Anthozoan *Cerianthus* sp. were identified by virtue of their

concentric rings of tentacles and a body size of about 10 mm (Leloup, 1964). The distribution of *Cerianthus* sp. larvae was virtually identical to that of the hydroids, but its abundance was considerably lower with a maximum average concentration of 50 m^{-3}. All 79 observations in Camera 2 showed these larvae positioned in a tentacle-down orientation.

Ctenophora (Fig. 6N)

The lobate ctenophore *Mnemiopsis* sp. was scattered throughout the water column on both the western and eastern sides of the channel. On the western side of the channel, individuals were observed on the Bank generally below 10 m in depth scattered in the WBW1 water. No major concentrations were associated with the front. There was a clear absence of ctenophores in the surface waters (CSW1, 2, 3, and PSW) above the thermocline. On the west side of the channel, ctenophores were found in the PIW-influenced region where maximum concentrations exceeded 250 m^{-3}. Body size ranged from 15 to >30 mm in diameter.

No preferred body orientation of *Mnemiopsis* sp. relative to the gravity vector was apparent. The ciliated comb plates, however, were observed to be beating on one side only as indicated by the presence of a metachronal wave. The side with beating comb plates was always on the underside of the animal when its body was rotated in one direction or another relative to the camera axis. This activity would tend to re-orient the animal to its vertical position (Moss and Tamm, 1986).

The cydippid ctenophore *Pleurobrachia* sp. was rare, with only a few observations in the PIW-influenced region at a depth of 30–40 m (data not shown). All 25 observations showed *Pleurobrachia* sp. to be in an upright posture (mouth down, apical sense organ up) with tentacles trailing to the side. Body size ranged from 8 to 12 mm in diameter.

T–S–P diagrams

The ability to assign characteristics of the physical environment to individual plankton enabled the creation of temperature–salinity–plankton (*T–S–P*) diagrams showing the relationship between plankton distributions and water mass structure at the individual level (Fig. 9). When Fig. 9 is compared with Fig. 4, it is clear that some taxa (e.g. *Limacina* sp., ophiopluteus larvae, *Obelia* sp.) exhibited well-defined boundaries related to a particular water mass, while others (e.g. *Calanus*) were scattered among and between water masses. As will be discussed later, this may be due to an interplay between the mobility of the plankton and the vertical stability of the water.

DISCUSSION

This study demonstrates a close association of plankton communities with water mass structure and distribution on scales of <1 m–70 km. The extent to which a given water mass acts as a boundary to a plankton assemblage is species-specific, with stronger constraints being imposed on less active organisms. When the actively swimming pteropods *Limacina retroversa* were constrained within a water mass, they concentrated at the center of the water parcel, rather than near any one boundary, and aggregated at small spatial scales. The copepod *Calanus finmarchicus*, however, was aggregated only in the thermocline. Conversely, concentrations of the more passive forms such as *Obelia* sp. and Ophiopleuteus larvae were greatest near boundaries and density interfaces, while their

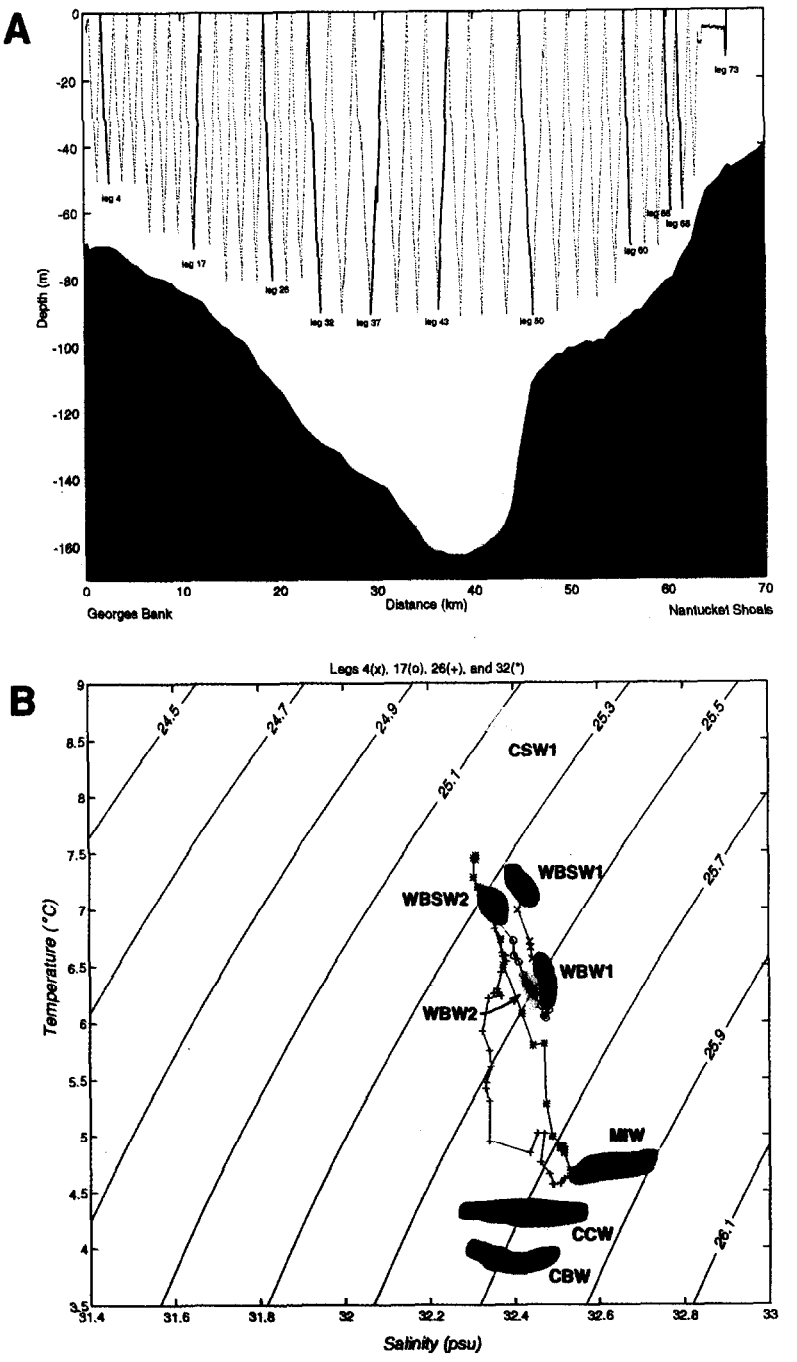

Fig. 3. Hydrographic data for VPR 22. (A) Towyo track of the VPR across Great South Channel (dotted line) with legs representing specific T–S properties (solid line) indexed by leg number. (B) T–S properties of legs 4 (×), 17 (○), 26 (+), and 32 (*). Identification of water types (colored areas) based on T–S data from all 74 legs of transect VPR 22. Outlines of water masses were drawn by hand. MIW: Maine Intermediate Water; SW: Surface Water; CCW: Cold Coastal Water; CBW: Cold Band Water; WBW1: Western Bank Water 1; WBSW1: Western Bank Surface Water 1; WBW2: Western Bank Water 2; WBSW2: Western Bank Surface Water 2; CSW1,2,3: Channel Surface Water 1,2,3; PSW: Plume Surface Water; PIW: Plume Intermediate Water.

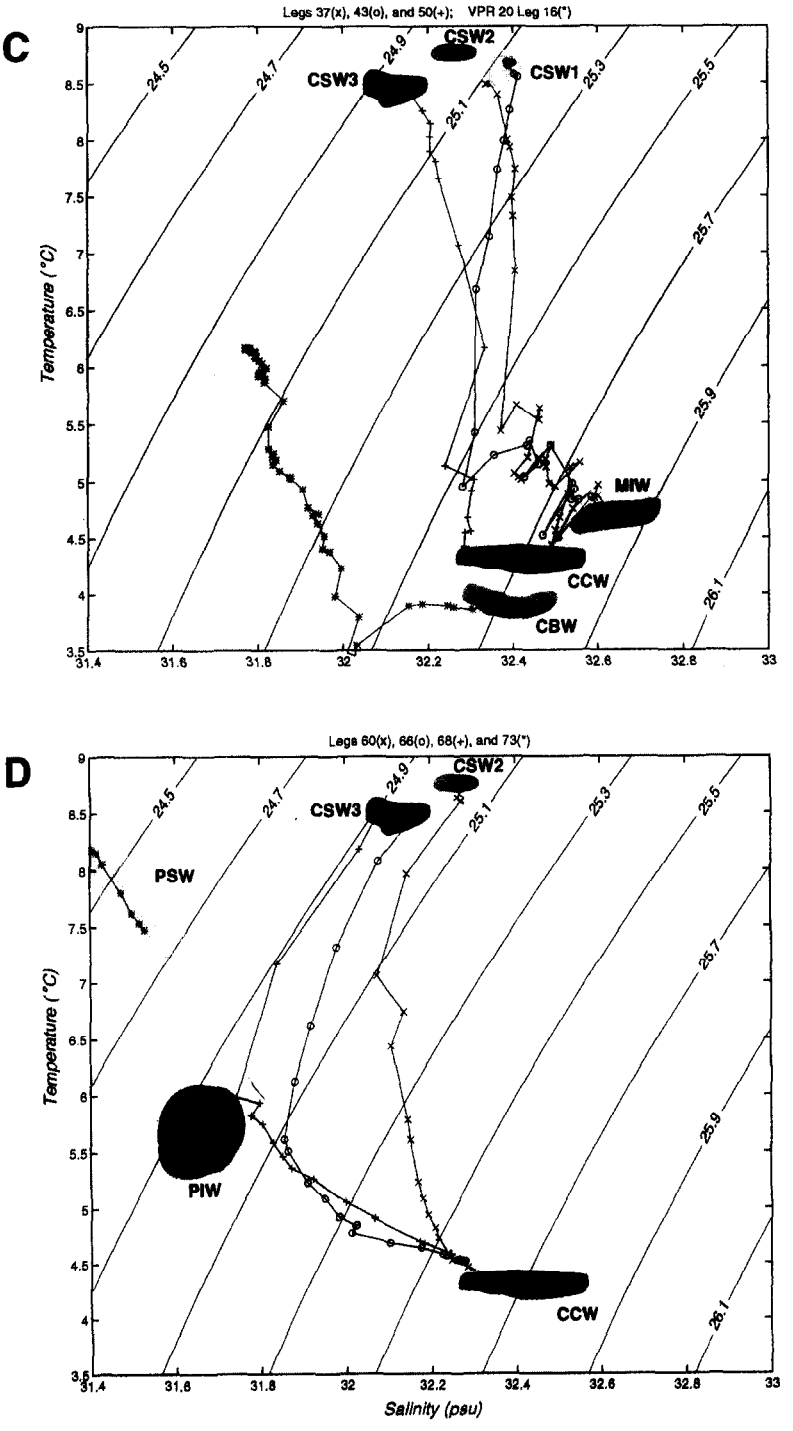

Fig. 3. (C) *T–S* properties of legs 37 (×), 43 (○), 50 (+), and VPR 20 leg 16 (*). (D) *T–S* properties of legs 60 (×), 66 (○), 68 (+), and 73 (*).

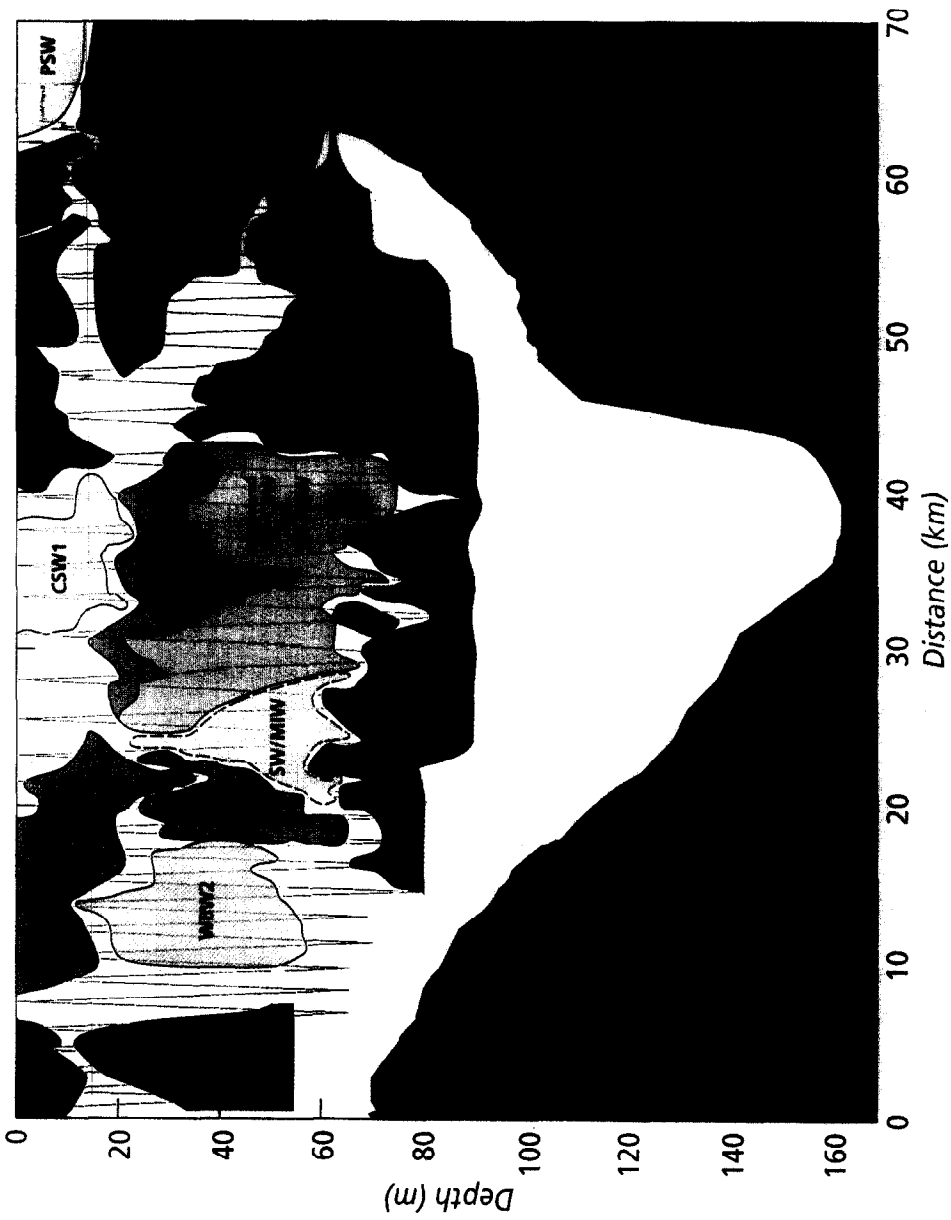

Fig. 4. Composite diagram of the vertical and horizontal distribution of water masses across the GSC based on T–S properties of identified water masses. All codes are as given in Fig. 3.

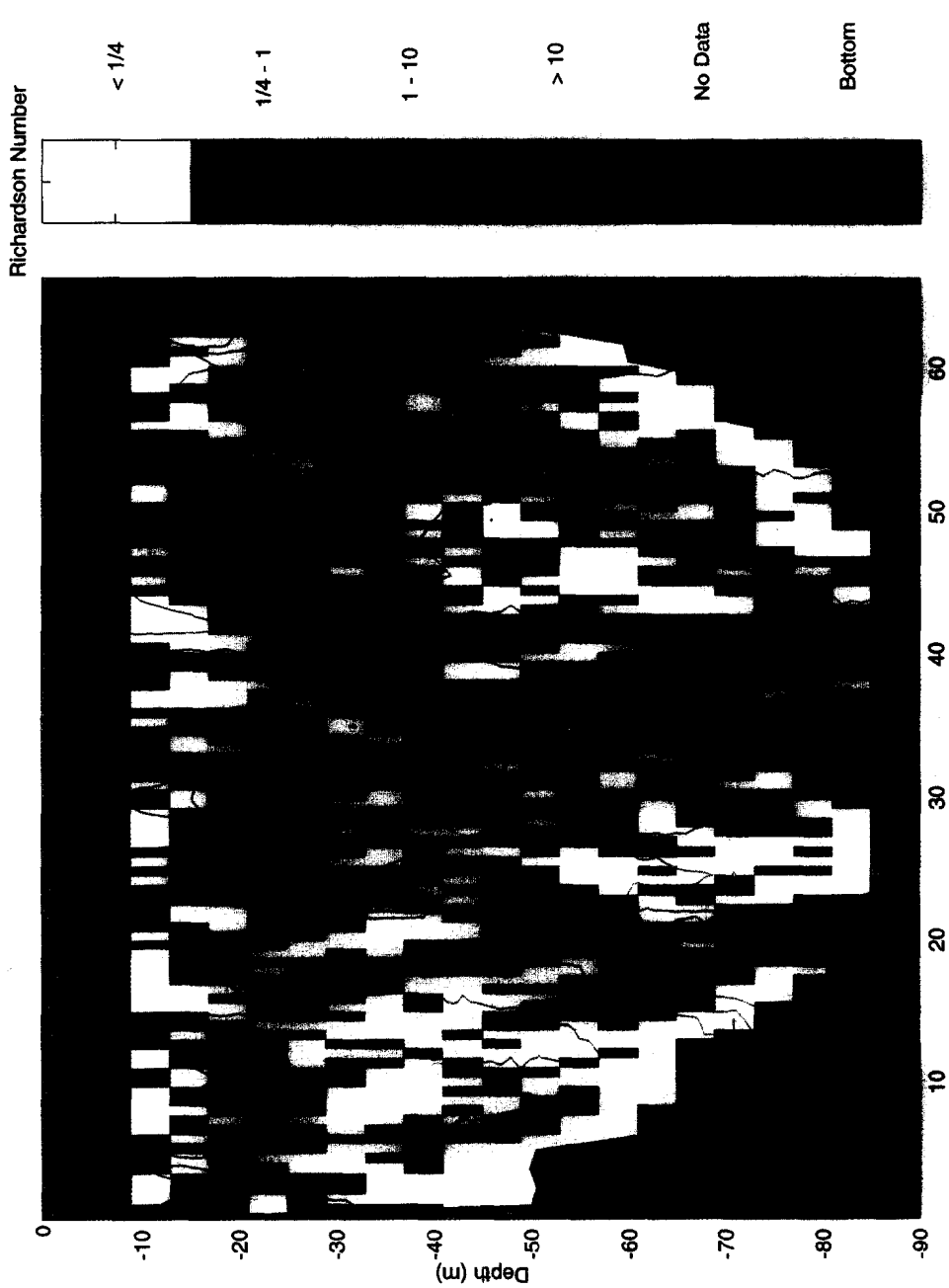

Fig. 5. Gradient Richardson number across Great South Channel calculated at intervals of 4 m depth by 600 m horizontal distance. White areas indicate $Ri < 0.25$; light blue areas indicate $0.25 < Ri < 1$; medium blue areas indicate $1 < Ri < 10$; and dark blue areas indicate $10 < Ri$. Contours of σ_t are overlaid for reference.

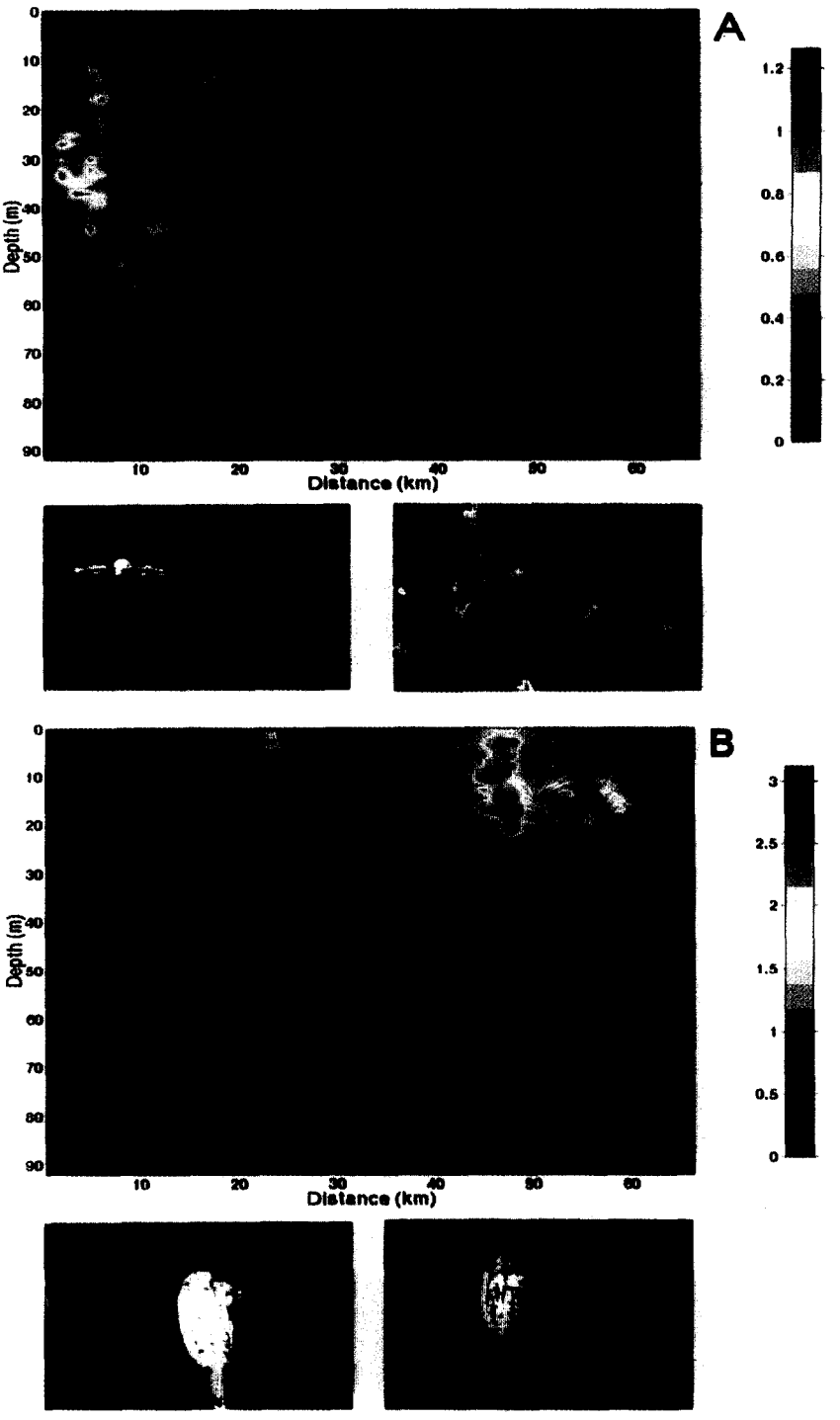

Fig. 6. Distribution and abundance (above) and two representative images extracted from the video tapes (below) of plankton identified along transect VPR 22. For figures (A),(B),(E),(F),(H),(I),(J),(K),(L),(M), and (N), data are from Camera 2 (field of view: 34 x 24.5 mm); for figures (C),(D), and (G), data are from Camera 4 (field of view: 6 x 4.4 mm). All images are from Camera 4. Temperature contours at 0.5°C intervals are overlaid for reference. (A) Hydroid medusa and polyp stages of *Obelia* sp., (B) *Calanus finmarchicus* CIV to adults.

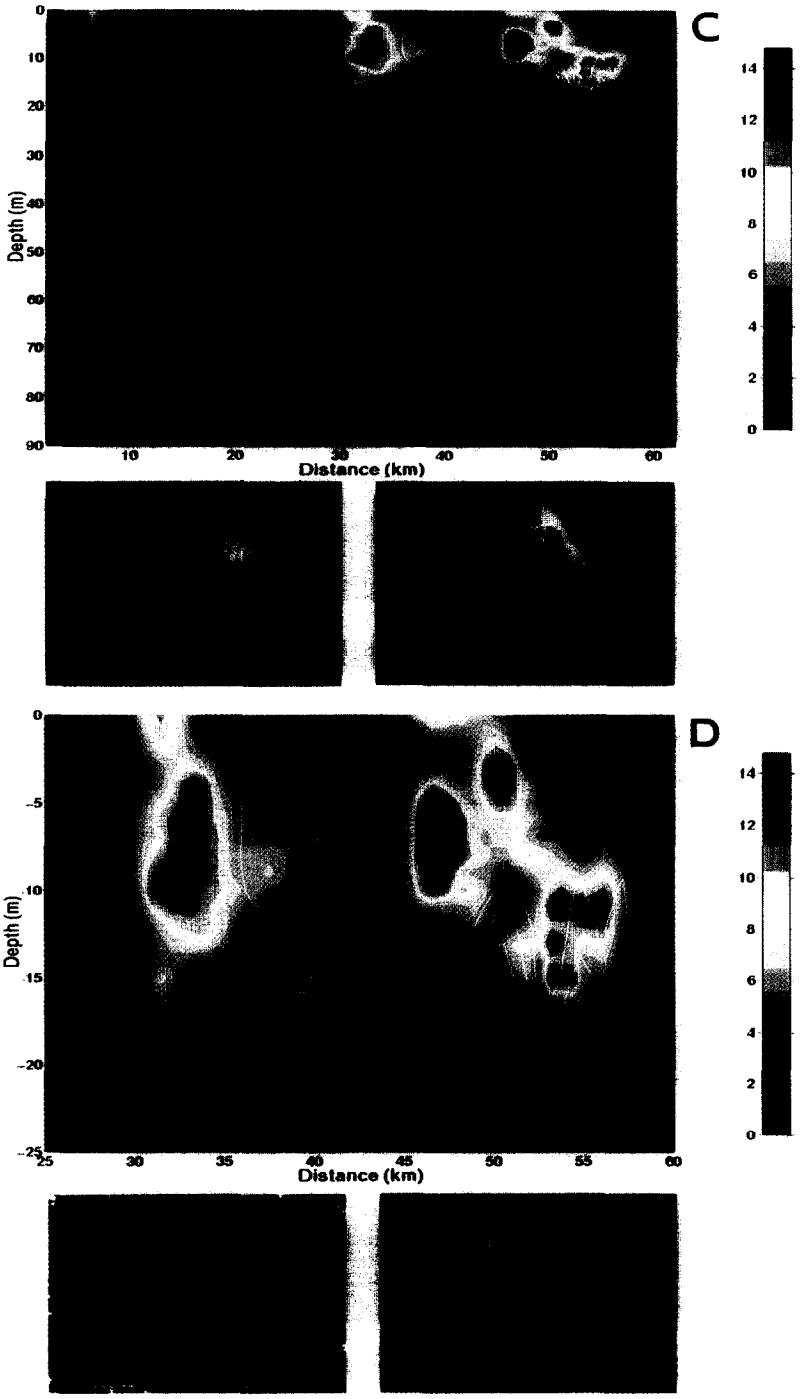

Fig. 6. (C) Pteropod *Limacina retroversa*, (D) two patches of *L. retroversa* located above the thermocline plotted on an enlarged scale. Note bounding of patches by 8.5°C temperature contour and the cloud of embryos being released by a pteropod in bottom left image.

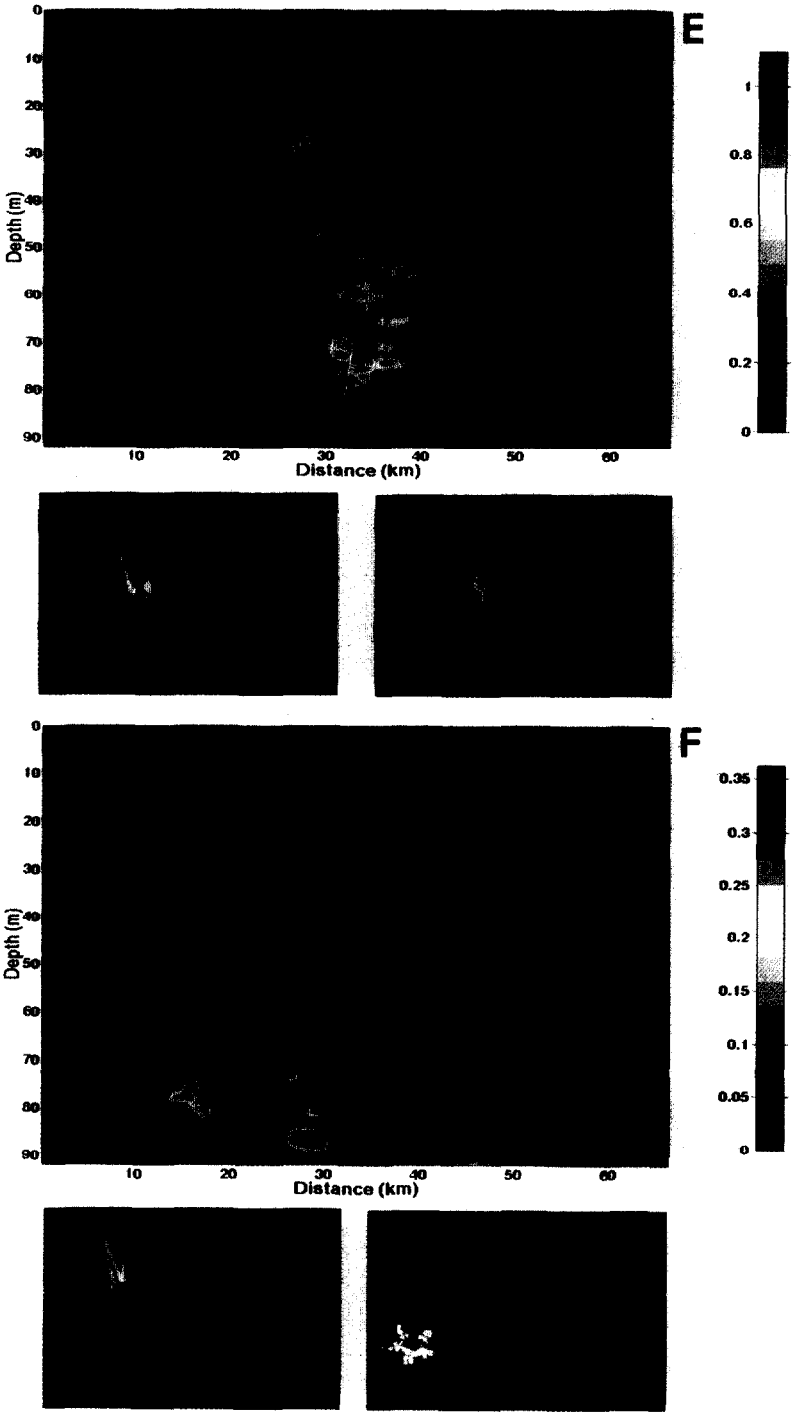

Fig. 6. (E) Ophiopluteus larvae, (F) ophiuroid juveniles.

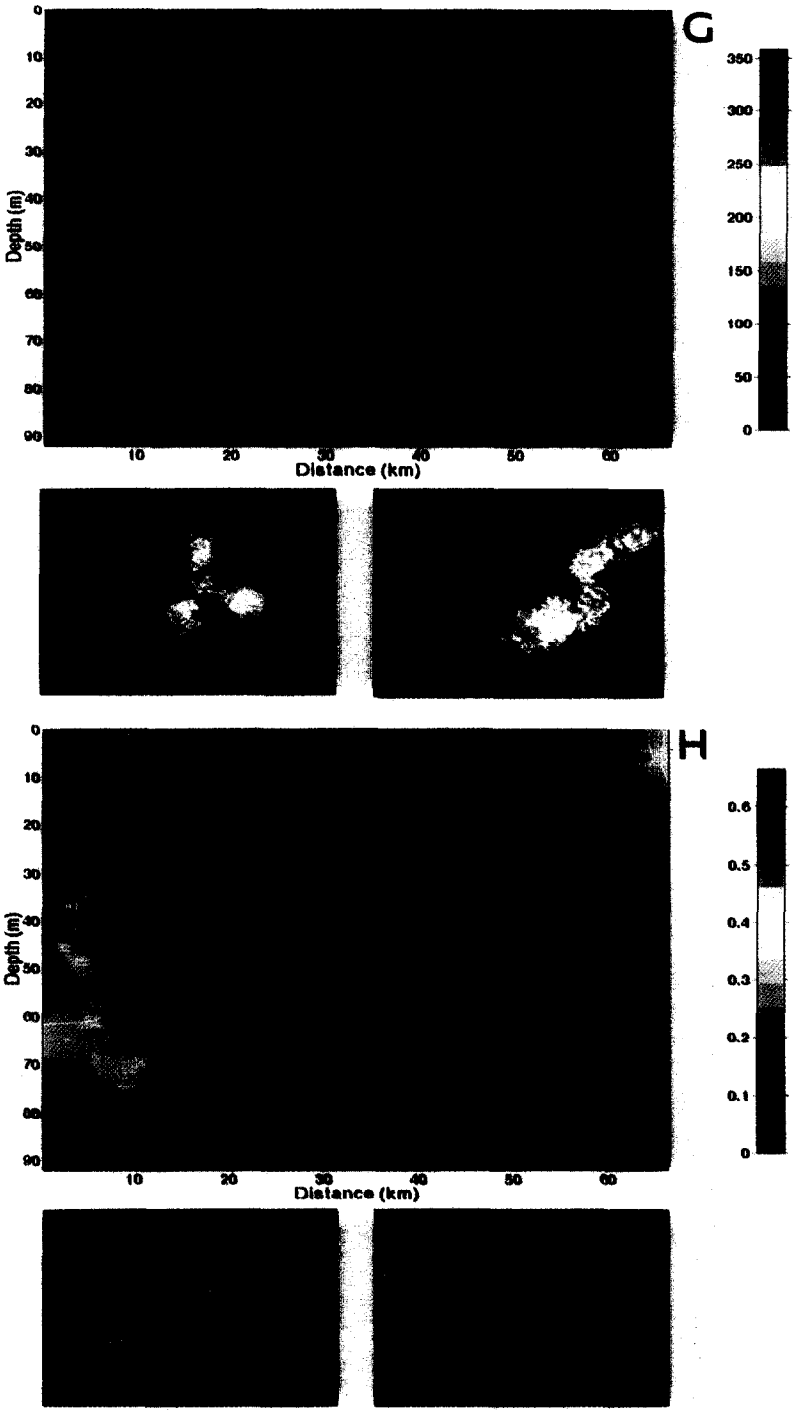

Fig. 6. (G) Colonial diatom *Chaetoceros socialis*, (H) larvaceans.

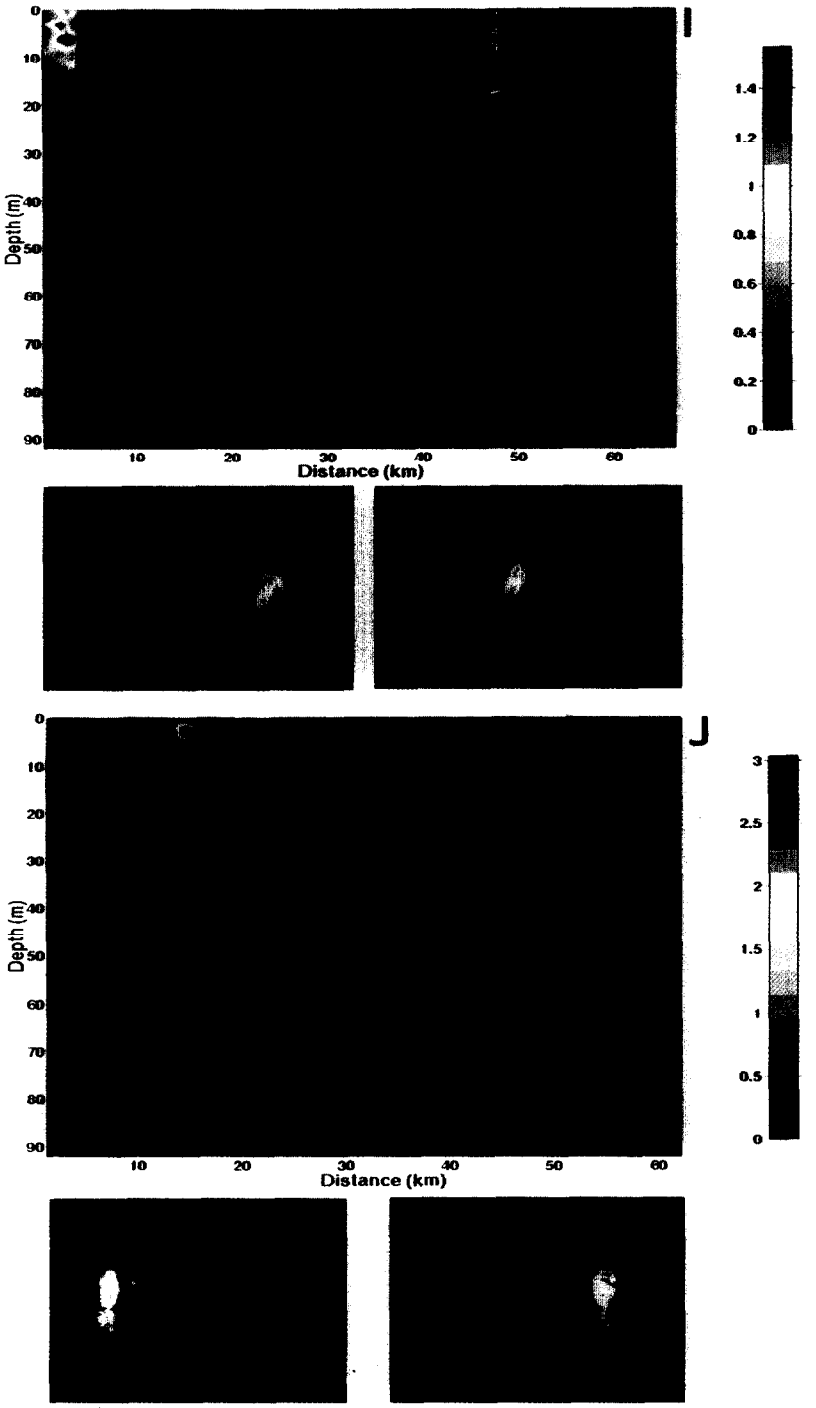

Fig. 6. (I) Other copepods, (J) gravid *Pseudocalanus* sp.

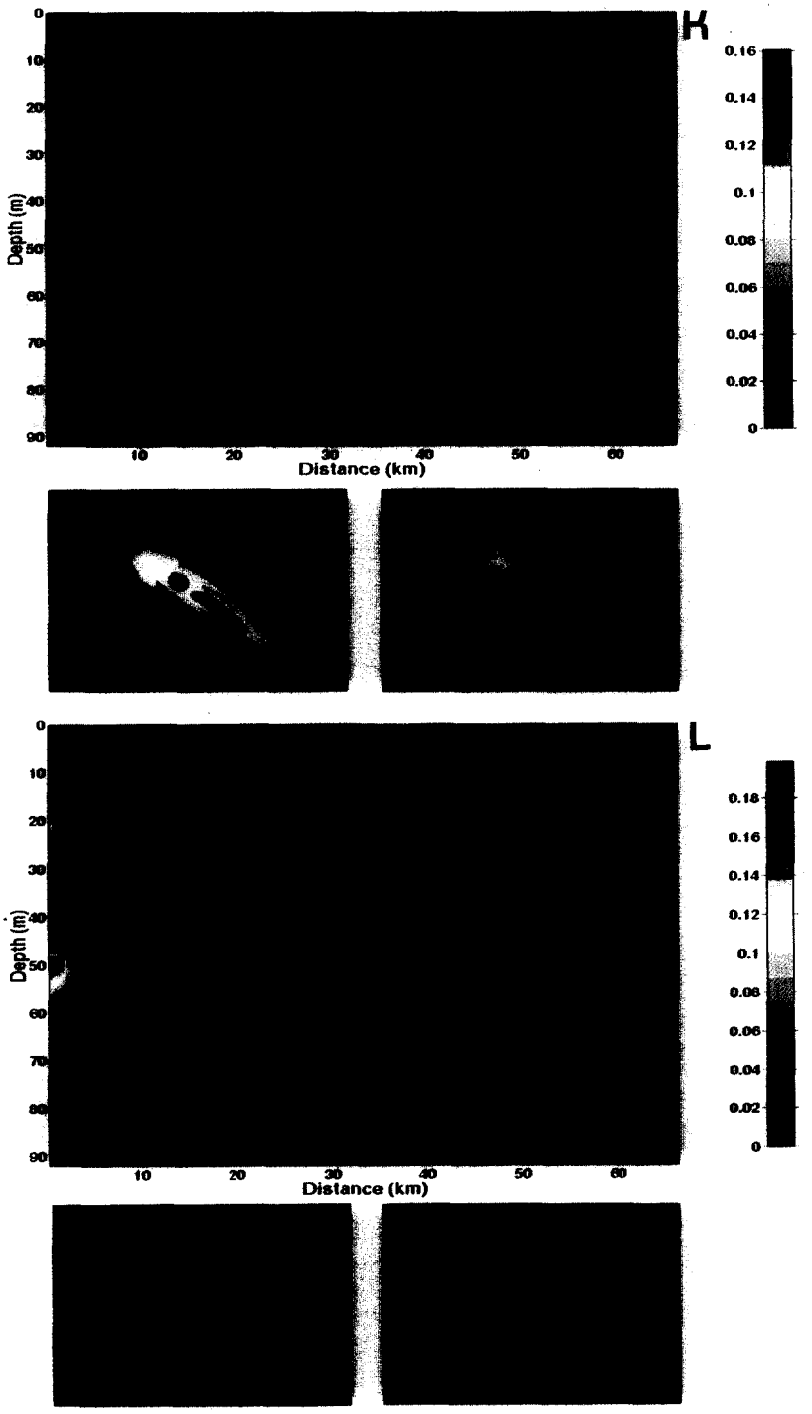

Fig. 6. (K) Pteropod *Clione* sp., (L) chaetognaths.

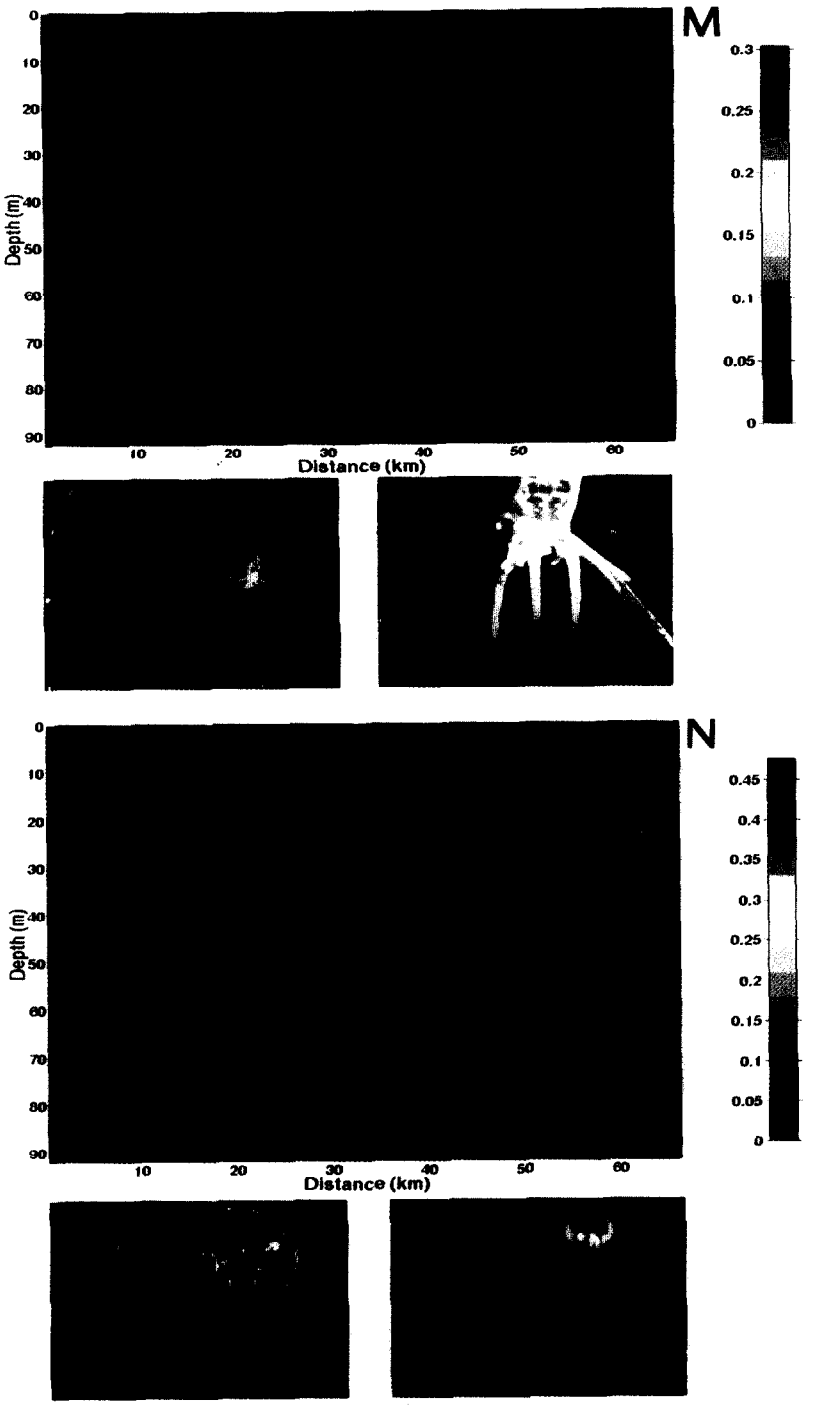

Fig. 6. (M) Larvae of *Cerianthis* sp., (N) ctenophores.

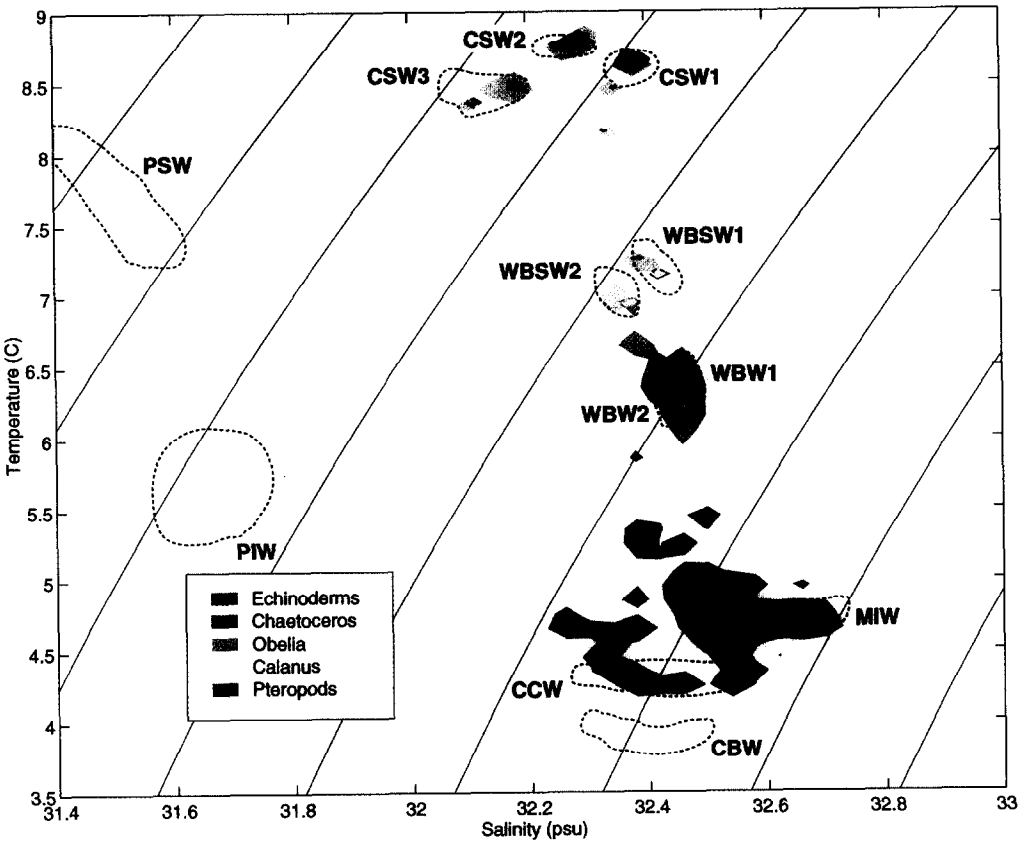

Fig. 9. Temperature–salinity–plankton (*T–S–P*) diagram showing the clustering of five plankton species as a function of the local *T* and *S*. Outlines (dashed lines) of water types from Fig. 3 are included for reference.

micro-scale distributions were more random. Taken together with water-column stability criterion as indicated by *Ri*, this suggests that weak swimmers tend to become concentrated in regions of high vertical stability (at edges of water masses or in density gradients) whereas more active plankton are able to aggregate either in regions of high vertical stability or relatively low stability (in center of water masses).

This study provides a high resolution, two-dimensional view of the mosaic of water types across the GSC. The complexity of the mosaic is due, in part, to interactions among the four distinct hydrographic regimes that converge in the northern Great South Channel: (i) the well-mixed Georges Bank crest water; (ii) the Gulf of Maine system; (iii) water overlying Nantucket Shoals; and (iv) water overlying the continental shelf and slope.

The general circulation pattern in the well-mixed region of Georges Bank is clockwise, flowing northward along the eastern side of the GSC. The plankton community of the well-mixed water was characterized by freely drifting hydroids (both colonial polyps and medusa of *Obelia* sp.), larvaceans, the colonial diatom *Chatoceros socialis*, ctenophores, larvae of the burrowing anthozoan *Cerianthus* sp. and scattered copepods. The western boundary of the Georges Bank water, the front between WBW2 and the region of MIW and mixed SW/CBW, coincides with a marked boundary in community structure. *Obelia* sp. medusa and cerianthid larvae were clearly bounded on the western side by the front while the larvaceans and ctenophores appeared on both sides of the channel. Bigelow (1926) discussed the presence of colonial hydroids in the water column being concentrated in frontal regions at the interface of well-mixed and stratified waters in the Gulf of Maine. Although these predominantly benthic forms may be scoured and resuspended from the bottom, as thought by Bigelow (1926), gonozooids, as well as gastrozooids with captured prey, were common in the VPR images, suggesting active reproduction and feeding in the water column. Thus, these hydroids may spend considerable time in the water column and be less transient than previously supposed.

Although adult burrowing anthozoans are fairly common in the deep basins of the Gulf of Maine (Theroux and Grosslein, 1987), cerianthid larvae have not been reported from plankton tows taken in the Georges Bank region. Perhaps this is because of damage by conventional sampling gear to their relatively soft and fragile bodies. Their tentacle-down orientation, even in the regions of high potential shear instability ($Ri < 0.25$) in the well-mixed area, suggests the existence of a strong torque induced by a center of gravity close to the tentacular region.

There are only a few references to the occurrence and distribution of *Chaetoceros socialis* in Gulf of Maine and Georges Bank region. Bigelow (1926) reported this colonial diatom to be the dominant phytoplankton species during the months of March and May in the well-mixed area. Falkowski and von Bock (1979) calculated the abundance of *C. socialis* to be 26% of the phytoplankton community in March. More recent observations of *C. socialis* in the western Gulf of Maine include those of Townsend *et al.* (1992) who reported colonies forming blooms in which chlorophyll *a* values exceeded 5 $\mu g\, l^{-1}$ during the month of April. On Georges Bank, recent reports of *C. socialis* are lacking except for observations made with the VPR throughout cruises EN237 in May 1992, CI9407 in May 1994, and EN267 in June 1995. During all three cruises, *C. socialis* occurred in great abundance along the northern and southern flanks as a subsurface chlorophyll maximum immediately below the pycnocline. Fluorometer readings exceeded 10 μg Chl $a\, l^{-1}$ while the video monitor turned white as the VPR traversed the diatom patches. Durbin *et al.* (1995a) reported that in May 1989 the GSC was dominated by large diatoms including *Rhizosolenia hebetata*, *Chaetoceros concavicornis*, *C. convolutus* and *Thalassiosira nordenskioldii*, but they did not

identify *C. socialis* in the SCOPEX studies (T. Durbin, personal communication, 1995). This may be explained by Bigelow's (1926) observation, that when *C. socialis* was present in the water column, plankton nets became covered in a slimy film, reducing their ability to filter small particles. The non-invasive sampling of the VPR proved useful in obtaining accurate estimates of population abundance and distribution for this important diatom.

In the central regions of the GSC, the population of ophiopluteus larvae was bounded vertically by the thermocline and the interface between MIW and SW/MIW, while the MIW contained virtually no larvae. Coincident with the distribution of ophiopluteus larvae in the central region of the GSC was a relatively low level of diatom colonies *Chaetoceros socialis* punctuated by extreme concentrations within the front. Before we examine the source of the larval and diatom populations, we must first consider the origins of the water mass in which they were embedded.

Judging by *T–S* properties alone, CCW mixed with surface water could provide the bulk of the water we have designated as SW/CBW. For this to be the case, however, the plume of CCW flowing south along the western side of the GSC would have to turn as it reached the sill, following the topography until it flowed northward along the eastern side of the GSC back towards the Gulf of Maine. In this scenario the CCW would mix tidally with surface water as it passed near the shallow GSC sill, producing, for example, the mixed surface water/cold water that is visible from about 30 to 60 m in depth between 20 and 40 km along the transect. A flaw in this scenario is that the sill of the GSC is about 70 m deep, and the mixed surface water/cold water is nearly all found above this depth. It seems unlikely that any CCW above 70 m would not simply pass over the sill of the GSC and thus exit the GSC/Gulf of Maine system.

In addition, the distribution of ophiopluteus larvae and colonial diatoms suggests that the CCW is not the source of this cold water. Extremely high concentrations of diatom colonies were found in the mixed surface water/cold water, yet the CCW itself was nearly devoid of diatom colonies and the surface waters of the central and western GSC contained virtually none. Perhaps the cold water came from some source outside the Gulf of Maine, and entered via the eastern GSC. One source candidate is the so-called Cold Band, a filament of cold water found on the south flank of Georges Bank during the spring, summer and early fall (Flagg, 1987). Transect VPR 20 was made across the south flank of Georges Bank (Fig. 1) two days before VPR 22. In the section described as Tow 4 in Norrbin *et al.* (1996), the Cold Band is visible as a temperature minimum between about 30 and 60 m deep. *T–S* diagrams for individual vertical legs of VPR 20 (Fig. 3c; Norrbin *et al.*, 1996) show that the Cold Band did indeed have *T–S* properties consistent with the cold water that was one ingredient of the mixed surface water/cold water found in VPR 22 across the GSC. As shown in Fig. 3, the Cold Band Water (CBW) had temperatures between about 3.75 and 4°C and salinities between about 32.3 and 32.5 psu. The Cold Band also contained high concentrations of diatom colonies (maximum $30\,l^{-1}$) and ophiopluteus larvae (maximum $11\,l^{-1}$) (Norrbin *et al.*, 1996), so it could have been a partial source for the diatoms and larvae found in the mixed surface water/cold water in VPR 22.

The kinematic picture we are thus suggesting (Fig. 10) shows the mid-depths of the central GSC occupied by a core of nearly stationary MIW and mixed surface water/MIW. On the eastern side of the GSC a plume of CCW flows southward past the MIW and crosses over the sill of the GSC. On the western side of the GSC, some of the water from the Cold Band is diverted from its general southwestward flow and crosses over the sill of the GSC, partially mixing with surface water there. When it reaches the core of the MIW and mixed SW/MIW,

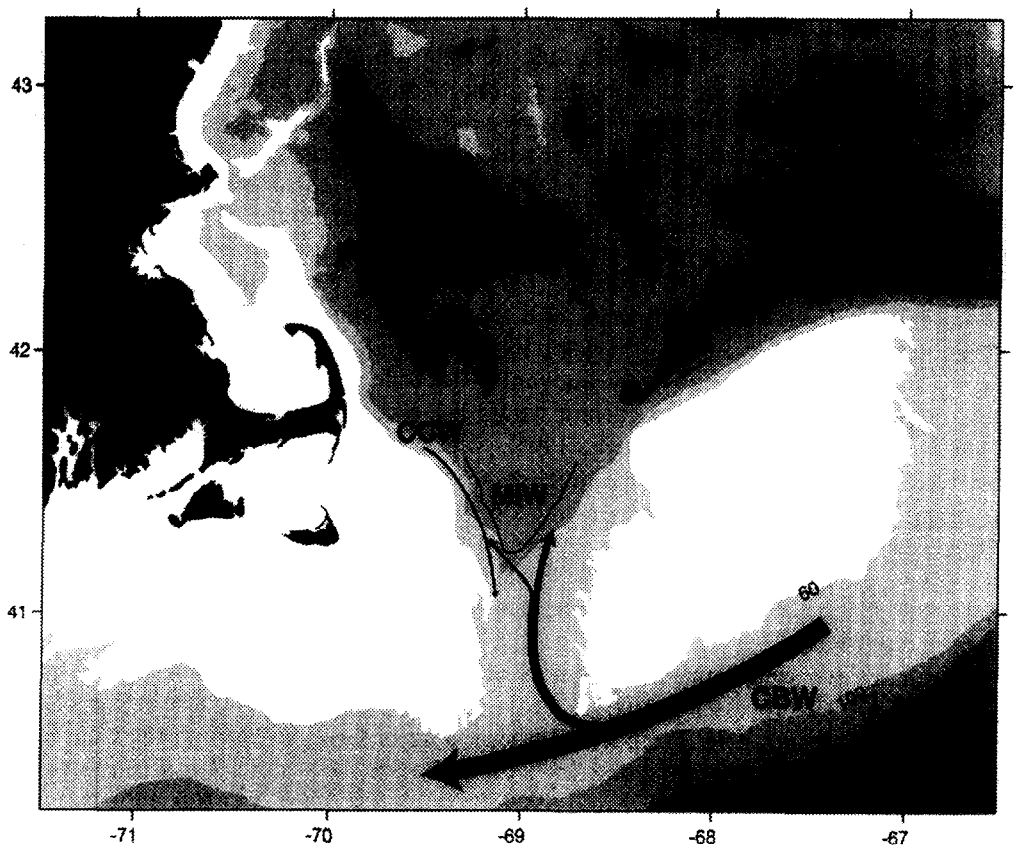

Fig. 10. Cartoon depicting implied flow occurring in the Great South Channel (GSC) during transect VPR 22. As Cold Band Water (CBW) flows southwestward along the south flank of Georges Bank, some water flows northward into the GSC, mixing with Maine Intermediate Water (MIW) and surface water. A tongue of Cold Coastal Water (CCW) moves south along the western rim of the GSC and past Nantucket Shoals. Deep MIW below the sill of the GSC moves south along the western edge of GSC turning to the north to follow topography of the western flank of Georges Bank. This kinematic picture is consistent with direct measurements in this region reported by Chen *et al.* (1995b).

the CBW/SW mixture divides: some of it flows northward in a thin jet between the WBW2 and the core of SW/MIW, and some of it flows northward to the west of that core, interleaving with the SW/MIW mixture as it progresses. This would explain how diatom colonies came to be distributed both east and west of the MIW and SW/MIW mixture, but it does not explain the dense concentration found in the front itself.

Aggregations of phytoplankton in fronts can be due to a combination of rapid growth, reduced grazing pressure, and physical concentration (Owen, 1981). Given the size of the *Chaetoceros socialis* colonies (>1 mm), direct grazing by all but the largest herbivores is probably not a consideration. Furthermore, the only zooplankton found in abundance in the region of the front were ophiopluteus larvae, which feed only on cells 10 μm or less in diameter (Strathmann, 1987). Thus grazing pressure on the colonies was probably low. Cell growth may have been fueled by a pool of relatively high levels of

ammonia and nitrate found at the base of the front in the 1988 and 1989 SCOPEX cruises by Durbin *et al.* (1995a). Although no data are available on the photosynthesis versus light intensity thresholds for this colonial form, many diatoms can be low-light adapted and form blooms below the pycnocline or at depth. Townsend *et al.* (1992) calculated the critical depth (the depth at which photosynthesis equals respiration) to be at 43 m in the western Gulf of Maine in April 1992 when *Chaetoceros* sp. dominated the water column. We should expect, therefore, that at least some growth, if not rapid growth, would be occurring while the colonies were in the frontal region. Furthermore, physical concentration of colonies in the front may have occurred through the interaction of down-welling currents and potentially buoyant cells. Some large cell masses have been observed to form gas bubbles internally (probably supersaturated O_2) causing them to become positively buoyant (Riebesell, 1992). The result of positively buoyant cells in a down-welling current would be to concentrate them along the length of the front (Franks, 1992; Epstein, 1995), which is consistent with the distribution observed here. Microscopic examination of *Chaetoceros socialis* colonies obtained on our recent cruise to Georges Bank in June 1995 (EN267) showed that most colonies had a large ($>100\,\mu m$) inclusion in the center of the cell mass. Whether this was a gas bubble or a solid body is unknown. Further studies on the physiology and growth kinetics of *C. socialis* need to be done before the mechanism(s) of concentration at fronts is elucidated.

The remarkably well defined boundaries of the ophiopluteus distribution could have been produced by processes similar to those controlling the distribution of the diatom colonies. Larvae transported from the southern flank of Georges Bank in the Cold Band water would be distributed to the east and west of the SW/MIW core. The *T–S* plots show interleaving between the SW/MIW and SW/CBW and SW/MIW, but this appears not to influence the larval distribution when the *T–S–P* plots are compared (i.e. few larvae were found in the SW/MIW core). Furthermore, the thermocline provided an upper boundary to the larval population, constraining them to the colder, more dense CBW and away from the surface CSW. Why are these boundaries so marked? Are the larvae depth-keeping and unable or unwilling to penetrate into the SW/MIW, MIW, and CSW1? Ophiopluteus larvae have relatively slow swimming speeds (*ca* $0.1\,mm\,s^{-1}$) compared with their much faster sinking speeds ($2–4\,mm\,s^{-1}$) (Konstantinova, 1966; Emlet, 1983), and are probably weak vertical migrators due to their apparent insensitivity to light (Mladenov and Chia, 1982). However, they should be able to keep their own depth, particularly since the water column appears reasonably stable in the region where the larvae are distributed ($Ri > 5$ on average). The unidirectional orientation of the larval body in all our observations is consistent with the idea of a relatively quiescent environment. Lack of penetration by the larvae through the thermocline and into the CSW1 could be caused by sensitivity to temperature, but why the larvae were not moving into the SW/MIW when the only significant gradient present was that of salinity is unknown. Working in the Kiel Bight, Banse (1964) noted that echinoderm larvae did not make excursions through the pycnocline and hypothesized that the larvae were "captured" in the water mass into which they were spawned. Larvae may be sensitive to salinity gradients and respond by sinking (reviewed by Young, 1995). However, the direct affects of changing kinematic viscosity with temperature and salinity on locomotory behavior in invertebrate larvae need closer attention before conclusions may be drawn concerning active or passive responses to physical gradients (Gallager *et al.*, 1996).

Equally interesting is the distribution of ophiuroids metamorphosing into the juvenile stage. The juvenile distribution appears as the inverse of the larval distribution (i.e. juveniles are found in abundance only in regions where larvae are not). Although we cannot find a description of planktonic metamorphosis in ophiuroids in the Gulf of Maine, juveniles have been observed from plankton samples collected from depth off the coast of New Hampshire (R. Olsen, personal communication, 1995). In our study, juveniles were found in water masses below those of the larval populations. Furthermore, some juveniles were observed in the well-mixed region to the east of the front in the virtual absence of larvae. Several explanations for this distribution include the following. Metamorphosing juveniles may cease swimming and, as they fall through the water column, develop to the point at which we staged them as juveniles from the video images. This does not explain, however, the sharp boundaries between larvae and juveniles which appear to coincide with our classification of water masses. Nor does it explain how juveniles appear to the east of the mixing front in the absence of larvae in the water column. Significant cross-frontal horizontal transport is possible where a tidal mixing front intersects the bottom (Owen, 1981). Perhaps cross-frontal transport coupled with downwelling along the front and recirculation up the sloping bottom produced the distributions reported here. Rapid transitions of temperature, salinity, or some other environmental constituent at the interface between water masses could provide the metamorphic cue triggering rapid advancement into the juvenile stage. This would result in larval stages being distributed in the central portions of water masses and metamorphosing juveniles at the edges. Alternatively, the larval population may have been at one time more or less uniformly distributed throughout the water column, including in the CCW, MIW and WBW water masses. Some environmental or biochemical constituent of the CCW, MIW and WBW water masses then could have triggered initiation of the metamorphic process. The result would be more developmentally advanced organisms in certain water masses and less advanced organisms in others. A final explanation may be that the larvae and juveniles are from different cohorts or even different species being transported differentially. In view of the previous discussion on the origins of the water masses, the idea that larvae were triggered to metamorphose at the interface between the CBW and SW/MIW seems most plausible.

The western GSC contained intrusions of cold, stratified water from the Gulf of Maine (Limeburner and Beardsley, 1982). The two groups of organisms most abundant in these waters were copepods, particularly *Calanus*, and the pteropod *Limacina retroversa*. *L. retroversa* was found in the water masses we call CSW1 and CSW2 but not in CSW3, whereas *Calanus* appeared scattered throughout CSW1 with a major aggregation extending from CSW3 into the thermocline.

High but variable concentrations of *L. retroversa* are common in the waters of the Gulf of Maine during late spring (Bigelow, 1926; Redfield, 1939). One population is believed to immigrate into the Gulf of Maine off the Scotian Shelf in December, and another appears in April (Redfield, 1939). Although growth and developmental rates for *L. retroversa* are unknown, it seems consistent that the gravid adult pteropods we observed spawning in the top few centimeters of the water column were immigrants to the Gulf of Maine while the resulting progeny were part of the second population appearing in the spring as discussed by Redfield (1939). Our observations also suggest these pteropods aggregate at the air–water interface at night for reproductive purposes, which is consistent with Redfield's observation that *L. retroversa* is a strong swimmer and vertical migrator from within the thermocline during the day to the surface at night.

The horizontal and vertical constraints placed on the pteropod population by the boundaries of CSW1 and CSW2 were remarkable. Concentrations averaged vertically over 1 m fell by a factor of 10 within a few meters of the 8.5° isotherm. Like most zooplankton, *L. retroversa* probably has little control over its horizontal movement, being transported passively within a water parcel. In addition, although it is a strong swimmer, with swimming speeds exceeding 10 cm s^{-1} and fall velocities ranging from 3 to 8 cm s^{-1} depending on size (Gallager, unpublished observations on shipboard), *L. retroversa* appeared to be constrained vertically at the base of the surface water overlying the thermocline. Unfortunately, we do not know the distribution of this pteropod during the day, but data from Redfield (1939) suggest it probably does not penetrate much deeper than the thermocline.

The GSC is known for its high abundance of *Calanus finmarchicus* during the spring (Bigelow, 1926; Wishner *et al.*, 1988 Wishner *et al.*, 1995), which attracts large numbers of right whales to the area at this time of the year (Wishner *et al.*, 1988, 1995). *C. finmarchicus* did not appear as constrained horizontally by water parcels as did *Limacina retroversa*, although the major copepod aggregations occurred to the west of the front. Of particular interest was a patch exceeding a concentration of 3 l^{-1} for a distance of about 5 km extending from within the thermocline to the surface. Similar patch dimensions for *C. finmarchicus* in GSC were described by Wishner *et al.* (1988, 1995), but their highest concentrations exceeded 40 l^{-1}. In the studies by Wishner *et al.* (1988, 1995), most copepods were CIV, suggesting a climax population preparing for diapause (Davis, 1987). The western edge of the patch appeared bounded by CSW2 while the eastern edge was abrupt within CSW3 without clear relationship to physical features. Wishner *et al.* (1988) discussed the various biological reasons for formation of a patch such as seen here, including aggregation in regions of high productivity, swarming by the use of mechanical and chemosensory communication, and predation. Without data on chlorophyll levels in the immediate vicinity of the patch, it is difficult to say if food was motivation for formation of the patch. Chlorophyll levels in the center of the patch described by Wishner *et al.* (1988) were low, suggesting either intense grazing by zooplankton or the termination of the spring bloom. The location of our transect VPR 22 and its hydrographic features are similar to that of transect D of the last leg of the SCOPEX cruise (Durbin *et al.*, 1995a) in June 1989. In the SCOPEX study, a sharp pycnocline at a depth of 15–20 m marked the boundary between low nutrients ($NO_3 < 0.25\ \mu M$, $NH_4 < 0.25\ \mu M$, $PO_4 < 0.3\ \mu M$, $SiO_2 < 1.0\ \mu M$) and chlorophyll (Chl $a < 1\ \mu g\ l^{-1}$) levels above, compared with a subsurface maxima for these variables just below the pycnocline ($NO_3 > 2.0\ \mu M$, $NH_4 > 2.0\ \mu M$, $PO_4 > 0.8\ \mu M$, $SiO_2 > 2.0\ \mu M$, Chl $a > 3\ \mu g\ l^{-1}$). Durbin *et al.* (1995b) found *Calanus finmarchicus* above the pycnocline to be food-limited and in generally poor condition, leading them to conclude that the low chlorophyll levels were a result of hydrographic and nutrient interactions rather than grazing by the copepods.

Another possible mechanism for formation of the *C. finmarchicus* patch found in this study is the interaction at density interfaces between internal waves and swimming behavior of the copepods. If *C. finmarchicus* sink into the thermocline during the day and become concentrated by internal wave activity (Haury *et al.*, 1983), migration to the surface as night approaches could occur in a tightly constrained patch. Internal waves are known to exist in this area at this time of the year, but confirmation of their existence in our study is lacking. Wishner *et al.* (1988) indicated that diurnal vertical migration in the population they studied was weak, so it is hard to speculate on the effect of internal waves without day-time

information from our transect. However, our data on micro-scale patchiness suggest *Calanus* was aggregating in regions of the water column where static stability was greatest. This is consistent with the idea that biological control of aggregation (swimming behavior) can dominate background physical mixing processes in regions of strong density gradients.

The final major hydrographic feature encountered during this transect was the surface plume of relatively fresh water in the western GSC that is believed to originate as river runoff. The VPR transect extended only about 5 km into this water mass. Larvaceans, ctenophores, pteropods and chaetognaths were common in this water mass and are known to inhabit this region at this time of the year (Bigelow, 1926).

CONCLUSIONS

Our analysis of transect VPR 22 over a distance of 62 km demonstrates the fine detail of biological and physical information that can be obtained using the VPR. It is clear that the GSC is a complex area both hydrographically and biologically, but that biological structure can be correlated to the hydrography over a wide range of spatial scales. Strikingly distinct distributions of plankton are bounded by specific water masses, which appear to provide impenetrable barriers both horizontally and vertically to both active and less mobile plankton. While coarse scale distributions are a function of hydrographic conditions, fine and micro-scale distributions appear related to the plankton's ability to aggregate in relation to background mixing intensity. Strong swimmers such as *Calanus finmarchicus* form dense clusters in regions where static stability of the water column is high, but are distributed randomly in regions were stability is low and the potential for mixing is higher. Conversely, another strong swimmer, *Limacina retroversa*, appeared contained and aggregated in the center of water masses that flowed in finger-like projections over cooler, denser water. The front between the well-mixed Georges Bank water and the mixture of CBW and surface water isolated a water parcel possibly originating from the southern flank of Georges Bank, in which diatom colonies bloomed over a relatively short time period. The distribution of metamorphosing ophiuroids at the base of the front suggests these hydrographic features are important for influencing the distribution of benthic invertebrates, and may be responsible for enhanced populations of certain species found around Georges Bank along the 60–70 m isobath (Theroux and Grosslein, 1987; Sinclair, 1988).

Acknowledgements—We thank Andy Girard, Ben Moten and Philip Alatalo for help in processing the video images, and Bob Elder and Craig Lewis for their efforts at sea in keeping the VPR in the water. This research was supported by NOAA MER Grant NA16RC0515–02, NSF GLOBEC Grant OCE-9313671, and ONR Grant N00014–93–1–0602. Contribution no. 8892 of the Woods Hole Oceanographic Institution. Contribution no. 61 of the U.S. Western Atlantic GLOBEC Program.

REFERENCES

Banse K. (1964) On the vertical distribution of zooplankton in the sea. *Progress in Oceanography*, **2**, 53–125.

Bigelow H. B. (1926) Plankton of the offshore waters of the Gulf of Maine. *Bulletin of the Bureau of Fisheries*, **40**, 1–509.

Bigelow H. B. (1927) Physical oceanography of the Gulf of Maine. *Bulletin of the Bureau Fisheries*, **40**, 511–1027.

Butman B. and R. C. Beardsley (1987) Long-term observations on the southern flank of Georges Bank: seasonal cycle of currents, temperature, stratification, and wind stress. *Journal of Physical Oceanography*, **17**, 367–384.

Cassie R. M. (1959) Some correlation in replicate plankton samples. *New Zealand Journal of Science*, **2**, 473–484.

Cassie R. M. (1960) Factors influencing the distribution pattern of plankton in the mixing zone between oceanic and harbor waters. *New Zealand Journal of Science*, **3**, 26–50.

Chen C., R. C. Beardsley and R. Limeburner (1995a) Variability of currents in late spring in the northern Great South Channel. *Continental Shelf Research*, **15**(4/5), 451–473.

Chen C., R. C. Beardsley and R. Limeburner (1995b) Variability of water properties in late spring in the northern Great South Channel. *Continental Shelf Research*, **15**, 415–431.

Cushing D. H. (1961) Patchiness. *ICES Rapp. Proc. Verb.*, **153**, 152–163.

Davis C. S. (1987) Zooplankton life cycles. In: *Georges Bank*, R. H. Backus, editor, MIT Press, Cambridge, MA, pp. 256–267.

Davis C. S., G. R. Flierl, P. H. Wiebe and P. J. S. Franks (1991) Micropatches, turbulence and recruitment in plankton. *Journal of Marine Research*, **49**, 109–151.

Davis C. S., S. M. Gallager, M. S. Burman, L. R. Haury and J. R. Strickler (1992a) The video plankton recorder (VPR): design and initial results. *Archiv fur Hydrobiologie, Beihefte, Ergebnisse der Limnologie*, **36**, 67–81.

Davis C. S., S. M. Gallager and A. Solow (1992b) Microaggregations of oceanic plankton observed by towed video microscopy. *Science*, **257**, 230–232.

Denman K. L. and D. L. Mackas (1977) Collection and analysis of underway data and related physical measurements. In: *Spatial pattern in plankton communities*, J. H. Steele, editor, Plenum Press, NY, pp. 85–110.

Denman K. L. and T. M. Powell (1984) Effects of physical processes on planktonic ecosystems in the coastal ocean. *Oceanography and Marine Biology Annual Review*, **22**, 125–168.

Durbin E. G., A. G. Durbin and R. C. Beardsley (1995a) Springtime nutrient and chlorophyll a concentrations in the southwestern Gulf of Maine. *Continental Shelf Research*, **15**, 433–450.

Durbin E. G., R. G. Campbell, S. L. Gilman and A. G. Durbin (1995b) Abundance, biomass, vertical migrations and estimated developmental rates of *Calanus finmarchicus* in the southern Gulf of Maine during late spring. *Continental Shelf Research*, **15**, 571–591.

Emlet R. B. (1983) Locomotion, drag, and the rigid skeleton of larval echinoderms. *Biology Bulletin*, **164**, 433–445.

Epstein A. W. (1995) Physical Processes and zooplankton distribution in the Great South Channel: observations and numerical studies. Ph.D. Thesis, 95–09, MIT/WHOI, MA.

Falkowski P. and K. von Bock (1979) Atlantic coastal experiment: phytoplankton species composition. Brookhaven National Laboratory Associated Universities, Inc. Report BNL-26335 USDOE, 266 pp.

Flagg C. N. (1987) Hydrographic structure and variability. In: *Georges Bank*, R. H. Backus, editor, MIT Press, Cambridge, MA, pp. 108–124.

Franks P. J. S. (1992) Sink or swim: accumulation of biomass at fronts. *Marine Ecology Progress Series*, **82**, 1–12.

Gallager S. M., J. L. Manuel, D. A. Manning and R. O'Dor (1996) Ontogenetic changes in the vertical distribution of scallop larvae *Placopecten magellanicus* in 9 m deep mesocosms as a function of light, food, and temperature. *Marine Biology*, **124**, 679–692.

Garrett C. J. R., J. R. Keeley and D. A. Greenberg (1978) Tidal mixing versus thermal stratification in the Bay of Funday and Gulf of Maine. *Atmosphere–Ocean*, **16**, 403–423.

Hardy A. C. and E. R. Gunther (1935) The plankton of the south Georgia whaling grounds and adjacent waters. *Discovery Reports*, **11**, 1–456.

Haury L. R. (1976) A comparison of zooplankton patterns in the California Current and North Pacific central gyre. *Marine Biology*, **37**, 159–167.

Haury L. R., J. A. McGowan and P. H. Wiebe (1978) Patterns and processes in the time-space scales of plankton distribution. In: *Spatial pattern in plankton communities*. J. H. Steele, editor, Plenum Press, New York, pp. 277–328.

Haury L. R., P. H. Wiebe, M. H. Orr and M. G. Briscoe (1983) Tidally generated high-frequency internal wave packets and their effects on plankton in Massachusetts Bay. *Journal of Marine Research*, **41**, 65–112.

Hopkins T. S. and N. Garfield (1979) Gulf of Maine Intermediate Water. *Journal of Marine Research*, **37**, 103–139.

Hopkins T. S. and N. Garfield (1981) Physical origins of Georges Bank water. *Journal of Marine Research*, **39**, 465–500.

Kann L. M. and K. Wishner (1995) Spatial and temporal patterns of zooplankton on baleen whale feeding grounds in the southern Gulf of Maine. *Journal of Plankton Research*, **17**, 235–262.

Konstantinova M. I. (1966) Characteristics of movement of pelagic larvae of marine invertebrates. *Dokl. Akad. Nauk. SSSR*, **170**, 726–729.

Leloup E. (1964) Larves de Cerianthaires. *Discovery Reports*, **33**, 251–307.

Limeburner R. and R. C. Beardsley (1982) The seasonal hydrography and circulation over Nantucket Shoals. *Journal of Marine Research*, **40**, 371–406.

Limeburner R. and R. C. Beardsley (1989) Lagrangian circulation in the Great South Channel and on Georges Bank during summer. In: *Proceedings of the third Georges Bank Research Workshop*. Bedford Institute of Oceanography, Bedford, Nova Scotia, Canada, 29 pp.

Mackas D. L., K. L. Denman and M. R. Abbott (1985) Plankton patchiness: biology in the physical vernacular. *Bulletin of Marine Science*, **37**, 652–674.

Marine Zooplankton Colloquium (1989) Future marine zooplankton research—a perspective, *Marine Ecology Progress Series*, **55**, 192–206.

McGowan J. A. (1967) Distributional atlas of pelagic mollusks in the California Current region. CalCOFI Atlas No. 6, State of California Research Committee.

McGowan J. A. (1974) The nature of marine ecosystems. In: *The biology of the Pacific Ocean*, C. B. Miller, editor, OSU Press, Corvallis, OR, pp. 9–28.

Michel H. B. and M. Foyo (1976) Caribbean Zooplankton. Part I. Siphonophora, Heteropoda, Copepods, Euphausiacea, Chaetognatha and Salpidae. Published by the Office of Naval Research, Library of Congress, no. 76–211–43.

Mladenov P. V. and F. S. Chia (1982) Development, settling behavior, metamorphosis and pentacrinoid feeding and growth of the feather star *Florometra serratissima*. *Marine Biology*, **73**, 309–323.

Moss A. G. and S. L. Tamm (1986) Electrophysiological control of ciliary motor responses in the ctenophore *Pleurobrachia*. *Journal of Computational Physiology*, **158**, 311–330.

Norrbin M. F., C. S. Davis and S. M. Gallager (1996) Differences in fine-scale structure and composition of zooplankton between mixed and stratified regions of Georges Bank. *Deep-Sea Research II*, **43**, 1905–1924.

Owen R. W. (1981) Fronts and eddies in the sea: mechanisms, interactions and biological effects. In: *Analysis of marine ecosystems*. A. R. Longhurst, editor, Academic Press, London, pp. 197–233.

Redfield A. C. (1939) The history of a population of *Limacina retroversa* during its drift across the Gulf of Maine. *Biological Bulletin*, **76**, 26–47.

Riebesell U. (1992) The formation of large marine snow and its sustained residence in surface waters. *Limnology and Oceanography*, **37**, 63–76.

Sinclair M. (1988) Marine populations: an essay on population regulation and speciation, Department of Fisheries and Oceans, Canada, 252 pp.

Steele J. H. (1976) Some comments on plankton patchiness. In: *Spatial pattern in plankton communities*. J. H. Steele, editor, Plenum Press, NY, pp. 1–20.

Strathmann R. R. (1987) Larval feeding. In: *Reproduction of marine invertebrates*. Blackwell Scientific, Palo Alto, CA, pp. 465–549.

Theroux R. and M. Grosslein (1987) Benthic Fauna. In: *Georges Bank*, R. Backus, editor, MIT Press, Cambridge, MA, pp. 283–295.

Townsend D. W., M. D. Keller, M. E. Sieracki and S. G. Ackleson (1992) Spring phytoplankton blooms in the absence of vertical water column stratification. *Nature*, **360**, 59–62.

Wiebe P. W. (1970) Small-scale spatial distribution in oceanic zooplankton. *Limnology and Oceanography*, **15**, 205–217.

Wiebe P. W., E. M. Hulbert, E. J. Carpenter, A. E. Cahn, G. P. Knapp, S. H. Boyd, P. B. Ortner and J. L. Cox (1976) Gulf Stream cold core rings: large scale interactions sites for open ocean plankton communities. *Deep-Sea Research I*, **23**, 695–710.

Wishner K., E. Durbin, A. Durbin, M. Macaulay, H. Winn and R. Kenney (1988) Copepods patches and right whales in the Great South Channel off New England. *Bulletin of Marine Science*, **43**, 825–844.

Wishner K., J. R. Schoenherr, R. Beardsley and C. Chen (1995) Abundance, distribution and population structure of the copepod *Calanus finmarchicus* in a springtime right whale feeding area in the southwestern Gulf of Maine. *Continental Shelf Research*, **15**, 475–507.

Young C. M. (1995) Behavior and locomotion during the dispersal phase of larval life. In: *Ecology of marine invertebrate larvae*, L. McEdward, editor, CRC Press, New York, pp. 249–278.